Mathematisches Forschungsinstitut Oberwolfach

Report No. 05/2011

DOI: 10.4171/OWR/2011/05

Mini-Workshop: Nonlinear Least Squares in Shape Identification Problems

Organised by
Marc Dambrine, Pau
Frank Hettlich, Karlsruhe
Roland Potthast, Berkshire

January 16th – January 22nd, 2011

Abstract. This mini-workshop brought together mathematicians engaged in shape optimization and in inverse problems in order to address a specific class of problems on the reconstruction of geometries. Such a problem can be formulated as an inverse problem forgetting the shape point of view or as minimization with respect to the shape.

Mathematics Subject Classification (2000): 49N45, 65N21.

Introduction by the Organisers

The workshop *Nonlinear Least Squares in Shape Identification Problems*, organised by Marc Dambrine (Pau), Frank Hettlich (Karlsruhe) and Roland Potthast (Berkshire) was held January 16th–January 22nd, 2011. This meeting was rather well attended with over 14 participants with strong european representation since it suffered late cancellations caused by the events in Tunisia. This workshop was a nice blend of researchers with various backgrounds and generated fruitful scientific discussions mixing different points of view.

The typical question addressed within the workshop is the inverse problem of determining an inclusion from measurements on the boundary of a domain. To that end, many strategies have been developed. Some approaches are based on shape optimization: for a guessed inclusion, considered as the variable, is associated a cost related to the measurements that has to be minimized. Some approaches are direct like the factorization method: a criterion is defined to check if a point belongs or not to the unknown inclusion. However, the problem is severely ill-posed: the unknown does not depend continuously on the measurements. Hence, every method has to face this difficulty and requires adapted regularization methods in order to find a numerical approximated solution.

The mini-workshop aimed at mixing people from different backgrounds using various methods to address the question of shape identification in order to discuss the connections between the approaches. Hence, the given talks can be grouped in three main themes:

- iterative methods based on a shape calculus for the detection of objects,
- direct methods for the detection,
- regularization methods for this inverse problem.

The first theme was covered by the presentations of Marc Dambrine, Eric Darrigrand, Helmut Harbrecht, Frank Hettlich, Barbara Kaltenbacher and Maria-Luisa Rapun. Furthermore, Corinna Burkard, Thomas Fiedler, Andreas Kirsch, Gen Nakamura and Roland Potthast were the speakers for the second theme. Finally, Barbara Kaltenbacher, Armin Lechleiter and Andreas Rieder gave talks on the last theme. Frédérique Le Louër gave a talk mixing both the first and third themes.

Some free discussion meetings were organized that allows the meeting participants to gather some open questions that seem of importance to the group and could be new research directions. For example, we discussed and selected among others the following questions:

- of the connections between the Radon transform of characteristic functions and the differentiation with respect to the domain,
- of recovering time-dependent objects; of shape derivatives for parabolic problems and for transmission problems,
- of obtaining convergence theories for dynamic Tikhonov regularization and for inexact Newton method under more reasonable assumptions,
- of the definition of resolution in electrical impedance tomography or in inverse scattering.

The organizers and participants of the mini-workshop are grateful to the *Mathematisches Forschunginstitut Oberwolfach* for providing a very pleasant and inspiring setting for the workshop allowing us to focus on the mathematical questions of importance.

Mini-Workshop: Nonlinear Least Squares in Shape Identification Problems

Table of Contents

Corinna Burkard (joint with Karim Ramdani)
The D.O.R.T. method for electromagnetic inclusions 205

Marc Dambrine
Stable and unstable problems in shape optimization 208

Eric Darrigrand (joint with Corinna Burkard, Marion Darbas, El-Hadji Koné, Frédérique Le Louër, Daniel Martin, Rania Rais)
Surface and Volume Integral Equations for the library MÉLINA++ 210

Thomas Fidler (joint with Markus Grasmair and Otmar Scherzer)
Shape Reconstruction based on Integral Invariants: An Inverse Problem 213

Helmut Harbrecht (joint with Karsten Eppler)
Shape Optimization for Free Boundary Problems 215

Frank Hettlich
The Domain Derivative of Time-Harmonic Electromagnetic Waves at Interfaces 218

Barbara Kaltenbacher
Shape sensitivities for a two problems in lithotripsy 219

Andreas Kirsch (joint with Andreas Kleefeld)
The Factorization Method for a Conductive Boundary Condition 222

Armin Lechleiter (joint with Andreas Rieder)
Newton Regularizations for EIT: The Complete Electrode Model and Convergence by Local Injectivity 223

Frédérique Le Louër (joint with Thorsten Hohage)
Regularized Newton methods for electromagnetic inverse obstacle scattering problems 225

Gen Nakamura
Inverse spectral problem for identifying damage in steel concrete composite beam; Active thermography and the dynamical probe method . 229

Roland W.E. Potthast
Mathematics and Application of Data Assimilation Algorithms 230

Roland W.E. Potthast
An Iterative Approach to Probe Methods 231

María-Luisa Rapún (joint with A. Carpio)
Topological derivatives for inverse scattering problems 233

Andreas Rieder (joint with Antonio Leitão)
`K-REGINN`: *An inexact Newton regularization of Kaczmarz type* 234

Abstracts

The D.O.R.T. method for electromagnetic inclusions

Corinna Burkard
(joint work with Karim Ramdani)

Based on the time-harmonic far field model for small dielectric inclusions in 3D, we study the so-called DORT method[1]. The main observation is to relate the eigenfunctions of the time-reversal operator to the location of small scattering inclusions. For non penetrable sound-soft acoustic scatterers, this observation has been rigorously proved for two and three dimensions by Hazard and Ramdani in [6] for small scatterers. In this talk, we consider the case of small dielectric inclusions with far field measurements. The main difference with the acoustic case is related to the magnetic permeability and the related polarization tensors. We show that in the regime $kd \to \infty$ (k denotes here the wavelength and d the minimal distance between the scatterers), each inhomogeneity gives rise to -at most- 4 eigenvalues (one due to the electric contrast and three to the magnetic one) while each corresponding eigenfunction generates an incident wave focusing selectively on one of the scatterers. Moreover, recent results concerning both the *closed* and the *open time-reversal mirror* are presented. The method has connections to the MUSIC algorithm known in Signal Processing and the Factorization Method of Kirsch ([7]).

1. Introduction

We consider a three-dimensional homogeneous electromagnetic medium described by a dielectric permittivity $\varepsilon_0 > 0$ and a magnetic permittivity $\mu_0 > 0$. The time dependence is supposed to be of the form $e^{-i\omega t}$ and will therefore be implicit. We assume that a local inhomogeneity is embedded in the above medium which is constituted of a collection of M homogeneous small imperfections of diameter δ and centers $\boldsymbol{s}_p \in \mathbb{R}^3$, $p = 1, \ldots, M$,

$$\mathcal{B}^\delta = \bigcup_{p=1}^{M} (\boldsymbol{s}_p + \delta \mathcal{B}_p),$$

where the reference inhomogeneity $\mathcal{B}_p \subset \mathbb{R}^3$, $p = 1, \ldots, M$ is a smooth and bounded domain containing the origin. We assume that $\varepsilon, \mu \in L^\infty(\mathbb{R}^3)$, $\inf_{\boldsymbol{x}\in\mathbb{R}^3} \varepsilon(\boldsymbol{x}) > \varepsilon_- > 0$ and $\inf_{\boldsymbol{x}\in\mathbb{R}^3} \mu(\boldsymbol{x}) > \mu_- > 0$ are respectively the real valued functions describing the dielectric permittivity and the magnetic permittivity of the perturbed medium. We assume that there exist positive constants (ε_p, μ_p), $p = 1, \ldots, M$, such that

$$\begin{cases} \varepsilon^\delta(\boldsymbol{x}) = \varepsilon_0, & \mu^\delta(\boldsymbol{x}) = \mu_0, \ \forall \boldsymbol{x} \in \mathbb{R}^3 \setminus \overline{\mathcal{B}^\delta}, \\ \varepsilon^\delta(\boldsymbol{x}) = \varepsilon_p, & \mu^\delta(\boldsymbol{x}) = \mu_p, \ \forall \boldsymbol{x} \in (\boldsymbol{s}_p + \delta \mathcal{B}_p). \end{cases}$$

[1]DORT is the French acronym for "Diagonalization of the Time Reversal Operator"

We further assume that the minimal distance $d := \min_{1\leq p<q\leq M} |\boldsymbol{s}_p - \boldsymbol{s}_q|$ is large compared to the wavelength $\lambda = \frac{2\pi}{k}$. We define respectively by $u^{\delta,\boldsymbol{\alpha}}$ and $v^{\delta,\boldsymbol{\alpha}}$ the total and scattered fields associated to the scattering problem of the incident plane wave $u_I^{\boldsymbol{\alpha}}(\boldsymbol{x}) := e^{ik\boldsymbol{\alpha}\cdot\boldsymbol{x}}$, $\boldsymbol{x} \in \mathbb{R}^3$, of direction $\boldsymbol{\alpha}$ by the small imperfections $\mathcal{B}^\delta$,

$$\operatorname{div}\left(\frac{1}{\mu^\delta}\nabla u^{\delta,\boldsymbol{\alpha}}\right) + \omega^2\varepsilon^\delta u^{\delta,\boldsymbol{\alpha}} = 0 \text{ in } \mathbb{R}^3, \text{ and } v^{\delta,\boldsymbol{\alpha}} := u^{\delta,\boldsymbol{\alpha}} - u_I^{\boldsymbol{\alpha}} \quad \text{is outgoing.}$$

The far field asymptotics of $v^{\delta,\boldsymbol{\alpha}}$ in the direction $\boldsymbol{\beta} \in S^2$ reads $v^{\delta,\boldsymbol{\alpha}}(\boldsymbol{\beta}|\boldsymbol{x}|) = e^{ik|\boldsymbol{x}|}/|\boldsymbol{x}|\, A^\delta(\boldsymbol{\alpha},\boldsymbol{\beta}) + O\left(1/|\boldsymbol{x}|^2\right)$, where $A^\delta(\boldsymbol{\alpha},\boldsymbol{\beta})$ is the scattering amplitude.

2. Selective focusing for closed time reversal mirrors

The results of this section are based on the far field asymptotics for the dielectric scattering problem, see the following Theorem (compare [1, Theorem 2]).

Theorem 2.1. *For all $p \in \{1,\ldots,M\}$, we set $\tilde{\mu}_p = \mu_0$ in $\mathbb{R}^3 \setminus \overline{\mathcal{B}_p}$ and $\tilde{\mu}_p = \mu_p$ in $\mathcal{B}_p$. Furthermore, let $\Phi_{p,j}$, for all $1 \leq j \leq 3$, be the unique solution of*

$$\operatorname{div}\left(\tilde{\mu}_p(\boldsymbol{x})\nabla\Phi_{p,j}(\boldsymbol{x})\right) = 0 \text{ in } \mathbb{R}^3, \quad \lim_{|\boldsymbol{x}|\to\infty} \Phi_{p,j}(\boldsymbol{x}) - x_j = 0.$$

Let $\mathbb{M}_p = (M^p_{i,j})_{1\leq i,j\leq 3}$ be the polarization tensor associated to the inhomogeneity $\mathcal{B}_p$ given by $M^p_{i,j} = \left(\frac{\mu_0}{\mu_p}\right)\int_{\mathcal{B}_p} \frac{\partial\Phi_{p,j}}{\partial x_i}\, d\boldsymbol{x}$, $\forall 1 \leq i,j \leq 3$. Then, as $\delta \to 0$, the scattering amplitude $A^\delta(\cdot,\cdot)$ admits the asymptotics $A^\delta(\boldsymbol{\alpha},\boldsymbol{\beta}) = \left(\frac{k^2}{4\pi}\right)\delta^3 A^0(\boldsymbol{\alpha},\boldsymbol{\beta}) + o(\delta^3)$, where

$$A^0(\boldsymbol{\alpha},\boldsymbol{\beta}) = \sum_{p=1}^{M} e^{ik(\boldsymbol{\alpha}-\boldsymbol{\beta})\cdot\boldsymbol{s}_p}\left[\left(\frac{\mu_p}{\mu_0} - 1\right)(\boldsymbol{\beta}\cdot\mathbb{M}_p\,\boldsymbol{\alpha}) - \left(\frac{\varepsilon_p}{\varepsilon_0} - 1\right)|\mathcal{B}_p|\right]. \tag{1}$$

The asymptotics holds uniformly for all $\boldsymbol{\alpha},\boldsymbol{\beta} \in S^2$.

By $F^0 : L^2(S^2) \longrightarrow L^2(S^2)$ we denote the integral operator corresponding to A^0, i.e. $F^0 f(\boldsymbol{\beta}) = \int_{S^2} A^0(\boldsymbol{\alpha},\boldsymbol{\beta})\, f(\boldsymbol{\alpha})\, d\boldsymbol{\alpha}$. By the representation formula of A^0 we obtain that F^0 is normal and thus the eigenfunctions of the time-reversal operator $T^0 = (F^0)^*F^0 = F^0(F^0)^*$ and F^0 are identical. Due to formula (1), F^0 has at most $4M$ eigenvalues since its range satisfies $\operatorname{Ran} F^0 \subset \bigoplus_{p=1}^M \operatorname{Span}\left\{e_p, \boldsymbol{\beta} \mapsto (\boldsymbol{\beta}\cdot C_p^j)\, e_p,\ j = 1,2,3\right\}$, in which $e_p(\boldsymbol{\beta}) = e^{-ik\boldsymbol{\beta}\cdot\boldsymbol{s}_p}$ and C_p^j, $j = 1,2,3$, denotes the column j of $\mathbb{M}_p$. We are now able to derive an expression for eigenfunctions of T in the regime $kd \to \infty$.

Theorem 2.2. *For all $p = 1,\ldots,M$, let $e_p \in L^2(S^2)$ be defined by $e_p(\boldsymbol{\alpha}) = e^{-ik\boldsymbol{\alpha}\cdot\boldsymbol{s}_p}$, and let $g_p \in L^2(S^2)$ be defined by $g_{p,\ell}(\boldsymbol{\alpha}) = h_{p,\ell}(\boldsymbol{\alpha})e_p(\boldsymbol{\alpha})$, $\ell = 1,2,3$, where the function $h_{p,\ell}$ is an eigenfunction (with eigenvalue $\zeta_{p,\ell}$) of the self-adjoint integral operator $\mathcal{M}_p \in \mathcal{L}(L^2(S^2))$ given by*

$$\mathcal{M}_p h(\boldsymbol{\beta}) := \int_{S^2} (\boldsymbol{\beta}\cdot\mathbb{M}_p\,\boldsymbol{\alpha})\, h(\boldsymbol{\alpha})\, d\boldsymbol{\alpha}.$$

We have the following two results.

(i) *As* $kd \to \infty$*, the functions* e_p *satisfy* $T^0 e_p = (\lambda_p^\varepsilon)^2 e_p + O\left((kd)^{-N}\right)$, $\forall N \in \mathbb{N}$, *with* $\lambda_p^\varepsilon = -4\pi\,(\varepsilon_p/\varepsilon_0 - 1)\,|\mathcal{B}_p|$.

(ii) *As* $kd \to \infty$*. the functions* $g_{p,\ell}$ *satisfy* $T^0 g_{p,\ell} = (\lambda_{p,\ell}^\mu)^2 g_{p,\ell} + O\left((kd)^{-N}\right)$, $\forall N \in \mathbb{N}$ *with* $\lambda_{p,\ell}^\mu = (\mu_p/\mu_0 - 1)\,\zeta_{p,\ell}$.

Given a fixed p in $\{1, \ldots, M\}$, let us consider the incident Herglotz associated with a density e_p, then

$$u_{I,p}(\boldsymbol{x}) = \int_{S^2} e^{ik\boldsymbol{\alpha}\cdot(\boldsymbol{x}-\boldsymbol{s}_p)}\,d\boldsymbol{\alpha} = 4\pi j_0(k|\boldsymbol{x}-\boldsymbol{s}_p|).$$

Since $j_0(s) = \sin(s)/s$, $s \in \mathbb{R}_+$, the incident field $u_{I,p}$ decreases like $1/\text{dist}(\boldsymbol{x}, \mathcal{B}_p)$.

Regarding the eigenfunctions $g_{p,\ell}$, the incident Herglotz wave is of the form

$$u_{I,p,\ell}(\boldsymbol{x}) = \int_{S^2} e^{ik\boldsymbol{\alpha}\cdot(\boldsymbol{x}-\boldsymbol{s}_p)} h_{p,\ell}(\boldsymbol{\alpha})\,d\boldsymbol{\alpha},$$

which is an oscillatory integral with function $h_{p,\ell}$. From the stationary phase theorem, it follows that for $kd \to \infty$, $u_{I,p,\ell} = O((kd)^{-N})$, $\forall N \in \mathbb{N}$. Thus, in both cases, the eigenfunctions corresponding to the scatterer p focus on s_p in the sense that the corresponding incident field decreases like $O((kd)^{-1})$ as $kd \to \infty$.

3. Remarks on selective focusing for open time reversal mirrors

The talk finishes with some observations concerning the open time reversal mirror (open TRM). First, we observe that the above theory is still valid for particular shapes of the TRM. Furthermore, shapes for the open TRM which can be used for selectively focussing properties seems to be connected to the polarization tensors.

Acknowledgements Support for this work was provided by the ANR MicroWave[2] and the FRAE (Fondation de Recherche pour l'Aéronautique et l'Espace)[3].

References

[1] H. Ammari, E. Iakovleva and S. Moskow, *Recovery of small inhomogeneities from the scattering amplitude at a fixed frequency*, SIAM J. Math. Anal., **34** (4) (2003), 882–900.

[2] X. Antoine, B. Pinçon, K. Ramdani and B. Thierry, *Far field modeling of electromagnetic time reversal and application to selective focusing on small scatterers*, SIAM J. Appl. Math., **69** (2008), 830–844.

[3] T. Arens, A. Lechleiter and R. D. Luke, *Music for extended scatterers as an instance of the factorization method*, SIAM J. Appl. Math., **70** (4) (2009), 1283-?1304.

[4] M. Fink and C. Prada, '*Acoustic time-reversal mirrors*, Inverse Problems, **17** (2001), 1761–1773.

[5] M. Fink, *Acoustic Time-Reversal Mirrors*, Chap. in Imaging of Complex Media with Acoustic and Seismic Waves, Topics in Applied Physics, **84** (2002), 17–43, Springer.

[6] C. Hazard and K. Ramdani, '*Selective acoustic focusing using time-harmonic reversal mirrors*, SIAM J. Appl. Math., **64** (2004), 1057–1076.

[7] A. Kirsch, *The factorization method for a class of inverse elliptic problems*, Math. Nachr., **278** (3) (2005), 258-?277.

[2]ANR-09-BLAN-0057-01: `http://microwave.math.cnrs.fr/`

[3]research project IPPON: `http://www.iecn.u-nancy.fr/~ramdani/IPPON`

[8] B. Pinçon and K. Ramdani, *Selective focusing on small scatterers in acoustic waveguides using time reversal mirrors*, Inverse Problems, **23** (2007), 1–25.

Stable and unstable problems in shape optimization

Marc Dambrine

The numerical procedures in shape optimization require a certain stability of the problem set at the continuous level. In order to establish that a minimizer is a local strict minimum of an objective function, the second order calculus is the natural tool. However, usually it turns out that its non negativeness is not sufficient to insure the stability. In classical optimization, the second order condition are stated as follows . If $f : E \to \mathbb{R}$ is $\mathcal{C}^2$ and $x \in E$ a minimizer of f, then Taylor-Young's formula at x provides

$$f(x+h) = f(x) + \frac{1}{2}D^2 f(x).[h,h] + o(\|h\|^2)$$

If $D^2f(x).[h,h]$ dominates $o(\|h\|^2)$, then f has a local strict minimum in x. This can be achieved by assuming that the hessian at the critical point $D^2f(x)$ is coercive. In shape optimisation the parameter $\mathbf{h}$ is a vector field generating a deformation of a domain. In this talk, I present the object shape hessian and explain on some examples how its sprectral properties affect the stability issue.

A first case encountered in eigenvalue optimization, magnetic shaping of liquid metal or optimal design for a mechanical structures is when the hessian is coercive. A significant example is the minimization of Dirichlet energy under a volume constraint. The problem can be written as : Find $\Omega^* = \text{argmin } J(\Omega)$ with

$$J(\Omega) = \frac{1}{2}\int_\Omega |\nabla u_\Omega|^2 - \int_\Omega k u_\Omega,$$

under the constraints supp $k \subset \Omega,\ |\Omega| = v$ and u_Ω solves the BVP

$$-\Delta u = k \text{ in } \Omega,\ u = 0 \text{ on } \partial\Omega.$$

At a critical shape of that problem, the hessian is

$$D^2J(\Omega).[\mathbf{h.n}, \mathbf{h.n}] = \mathbf{2}\lambda \int_{\partial\boldsymbol{\Omega}} \mathbf{h.n}\ \boldsymbol{\Lambda}(\mathbf{h.n}) + \mathbf{H}(\mathbf{h.n})^{\mathbf{2}};$$

where λ is the Lagrange multiplier of the volume constraint, H is the mean curvature of $\partial\Omega$ and Λ is the Dirichlet-to-Neumann operator $\mathrm{H}^{1/2}(\partial\Omega) \to \mathrm{H}^{-1/2}(\partial\Omega)$. When Ω convex for instance, it holds

$$D^2J(\Omega).[\mathbf{h.n}, \mathbf{h.n}] \geq \mathbf{C}\|\mathbf{h.n}\|^{\mathbf{2}}_{\mathrm{H}^{\mathbf{1/2}}(\partial\boldsymbol{\Omega})}$$

but, in Taylor's formula $o(\|\mathbf{h.n}\|^{\mathbf{2}}_{\mathcal{C}^{\mathbf{2}}(\partial\boldsymbol{\Omega})})$ occurs. A two norm discrepancy problem appears: the hessian in coercive for a weak norm $(\|.\|_{\mathrm{H}^{1/2}(\partial\Omega)})$ with respect the norm of differentiability $(\|.\|_{\mathcal{C}^2(\partial\Omega)})$. In this particular case, it can be overcome thanks to the continuty result for the shape hessian proved in [1]. There are $\eta_0 > 0$ and a modulus of continuity $\omega : (0, \eta_0] \to (0, +\infty)$ such that $\forall \eta \in (0, \eta_0]$ and

$\forall\Theta \in \mathcal{C}^{2,\alpha}$ with $\|\Theta - Id\|_{2,\alpha} \leq \eta$ diffeomorphism $\mathbb{R}^d \to \mathbb{R}^d$, there is a deformation field $\mathbf{h}[\Theta]$ such that

$$|e''_\Theta(t) - e''_\Theta(0)| \leq \omega(\eta)\|bfh[\Theta].\mathbf{n}\|^2_{\mathrm{H}^{1/2}(\partial\Omega)}$$

with $e(t) = E(\Phi_{\Theta,t}(\Omega_0))$. Then, a weakly coercive hessian insures stability and K. Eppler, H. Harbrecht and R. Schneider have shown a corresponding result for the associated numerical scheme([2]).

A worst case appears when using least squares type (or Kohn-Vogelius like) objective functions to recover inclusion(s) ω inside a domain Ω from measurements made on the boundary $\partial\Omega$. For example, if a perfectly insulating inclusion is to be detected, the problem can be written as: Find ω such that the overdetermined boundary value problem

$$\begin{aligned} -\Delta u &= 0 \text{ in } \Omega \setminus \overline{\omega}, \\ u &= f \text{ on } \partial\Omega, \\ \partial_n u &= g \text{ on } \partial\Omega, \\ \partial_n u &= 0 \text{ on } \partial\omega, \end{aligned}$$

has a solution. A Least Squares formulation is to find ω that minimizes

$$J_{LS}(\omega) = \frac{1}{2}\int_{\partial\Omega} |u_N - f|^2;$$

where the state u_N is harmonic in $\Omega \setminus \overline{\omega}$ with the boundary conditions $\partial_n u_N = g$ on $\partial\Omega$, $\partial_n u_N = 0$ on $\partial\omega$ and a normalization condition is imposed. When ([3]) one computes the hessian at a critical shape ω^*, one gets

$$D^2 J_{LS}(\omega^*).[\mathbf{h},\mathbf{h}] = \int_{\partial\Omega} (u'_N)^2.$$

This is a square, it is non negative so we could expect stability but the dependency in the right parameter $\mathbf{h}$, the deformation field, is not explicit. Once it is explicited, one checks that the Riesz representative $\mathrm{H}^{1/2}(\partial\omega^*) \to \mathrm{H}^{-1/2}(\partial\omega^*)$ of the hessian $D^2 J_{LS}(\omega^*)$ is compact. In particular, the hessian is not coercive.

To understand what compactness means here, let us take the example of a starshaped domain ω in dimension two. Assume that $\partial\omega$ is parametrized by

$$\partial\omega = \left\{ \begin{pmatrix} g_0 \\ g_1 \end{pmatrix} + \left(g_2 + \sum_{k=1}^{\infty} (g_{2k+1}\cos(k\,t) + g_{2k+2}\sin(k\,t)) \right) \begin{pmatrix} \cos(t) \\ \sin(t) \end{pmatrix} \right.$$
$$\left. = \sum_{k=0}^{\infty} g_k \mathbf{h}_k(t);\ t \in (0, 2\pi) \right\},$$

Then, for all $n \in \mathbb{N}$, $\exists C_n > 0$

$$\forall \mathbf{h} \in \mathrm{Span}(\mathbf{h}_k)_{0 \leq k \leq 2n+2},\ D^2 J(\omega^*) \cdot (\mathbf{h},\mathbf{h}) \geq C_n\,|\mathbf{h}|^2,$$

but $C_n \to 0$ which explains the numerical need for regularization and for the methods developed by the inverse problem community. Such a situation is generic in geometrical inverse problem and can also be encountered in some optimal design problem in mechanical engineering [4].

References

[1] M. Dambrine, *On variations of the shape Hessian and sufficient conditions for the stability of critical shapes.* RACSAM Rev. R. Acad. Cienc. Exactas F?s. Nat. Ser. A Mat. 96 (2002), no. 1, 95?121.

[2] K. Eppler, H. Harbrecht and R. Schneider. *On convergence in elliptic shape optimization.* SIAM J. Control Optim. 46 (2007), no. 1, 61?83.

[3] L. Afraites, M. D., K. Eppler, D. Kateb, *Detecting perfectly insulated obstacles by shape optimization techniques of order two.* DCDS Ser. B 8 (2007), no. 2, 389?416

[4] M. Dambrine and D. Kateb. *On the ersatz material approximation in level-set methods.* ESAIM Control Optim. Calc. Var., 16(3):618 ? 634, 2010.

Surface and Volume Integral Equations for the library Mélina++

Eric Darrigrand

(joint work with Corinna Burkard, Marion Darbas, El-Hadji Koné, Frédérique Le Louër, Daniel Martin, Rania Rais)

Inverse scattering problems and antennas design are fields that also require the consideration of the related direct problem which is in our case wave propagation in exterior domains. This subject has been solved using many different strategies like finite elements using an artificial boundary or integral equations or combinations of both volume finite elements and integral representations.

The library Mélina++ ([1]) has been developed mainly by Daniel Martin at the university of Rennes 1. Mélina++ is a free Finite Element library organized such that the user only needs to write a main function that describes the variational formulation of the problem to be solved. The library can be extended to almost any equation that admits a Galerkin discretization. In particular, the usual surface and volume integral operators were integrated in Mélina++ in order to enable one to deal with any of the following strategies for the resolution of scattering direct problems:

- Coupling of volume finite elements and integral representation.
- Surface integral equations.
- Volume integral equations.

In the following, we then describe three techniques that were implemented or that are under implementation using the library Mélina++ for the resolution of the direct problem related to acoustic or electromagnetic wave propagation. A first example explains the coupling of volume finite elements and integral representation. A second one shows a preconditioning strategy for the surface integral equation based on On Surface Radiation Conditions (OSRC). The last example concerns a volume integral equation considered within lens-antenna design.

As a first example, we consider the Helmholtz equation in exterior domain Ω delimited by the boundary Γ of an obstacle and an artificial boundary Σ.

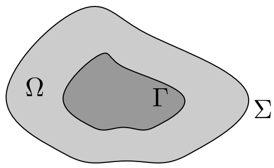

With k the wavenumber, $u^{\rm inc}$ the incident wave and $G(x,y) = \frac{e^{ik|x-y|}}{4\pi|x-y|}$ the Helmholtz fundamental solution, we solve the following problem with $f = -\partial_n u^{\rm inc}|_\Gamma$:

$$\begin{cases} \Delta u + k^2 u = 0 \quad \text{in } \Omega, \\ \partial_n u = f \quad \text{on } \Gamma, \\ (\partial_n - ik)u(x) = (\partial_n - ik) \displaystyle\int_\Gamma \big(u(y)\partial_{n_y} G(x,y) - f(y)G(x,y)\big)\, ds(y) \quad \text{on } \Sigma. \end{cases}$$

by using a combination of Finite Elements on the volume Ω and an integral representation based on Jami and Lenoir work ([2]). The integral representation expresses the unknown on Σ from itself on Γ and gives an exact condition on the artificial boundary. A current work with N. Gmati, D. Martin and R. Rais, consists in studing the resolution of this problem as a Schwarz algorithm ([3]) and establishing the impact of the Fast Multipole Method applied to this configuration. This example involves the library MÉLINA++ which provides with integrands like:

$$ik \int_\Sigma \int_\Gamma u(y)\partial_{n_y} G(x,y) ds(y) \overline{v}(x) ds(x)$$

defined thanks to MÉLINA++ command:
`NVTermMatrix nDyGF(Gamma,u_h,Sigma,u_h, ngrady(GF),"nDyGF");`
Here `u_h` defines the unknown discretization and `GF` is the Green function.

A second example is the Brakhage-Werner integral formulation

$$\left(\frac{1}{2} - K - \eta D\right) \varphi = -\partial_n u^{\rm inc}|_\Gamma \qquad \text{on } \Gamma$$

where

$$K\varphi(x) = \int_\Gamma \partial_{n_y} G(x,y)\varphi(y) ds(y) \ \text{ and } \ D\varphi(x) = -\int_\Gamma \partial_{n_x}\partial_{n_y} G(x,y)\varphi(y) ds(y)\,.$$

This formulation is used for the resolution of the exterior Helmholtz equation around the obstacle Ω^- of boundary Γ defined in the following picture

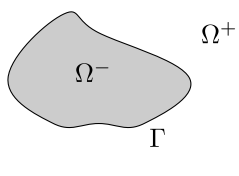

and where the incident field is denoted by u^{inc}. A preconditioned version was established by X. Antoine and M. Darbas ([4]) using OSRC techniques:

$$\left(\frac{1}{2} - K - D\widetilde{V}\right)\varphi = -\partial_n u^{\mathrm{inc}}|_\Gamma \qquad \text{on } \Gamma$$

where $\widetilde{V}$ is a local approximation to the Neumann-to-Dirichlet operator. The technique leads to an efficient preconditioning of the integral equation and gives impressive numerical results. It can be interpreted as a generalization of the choice of an optimal parameter for the Brakhage-Werner integral formulation due to R. Kress: $\widetilde{V} = \eta_{\mathrm{opt}} = -i/k$. A work in progress with M. Darbas will involve the library MÉLINA++ in order to investigate the impact of the Fast Multipole Method when it is applied to this context and make sure that it does not reduce the preconditioning. MÉLINA++ is used with the following objects:

```
IEMTermMatrix K(Gamma, u_h, u_h, ngrady(GF));
IEMTermMatrix Dnn(Gamma, nx(u_h), nx(u_h), GF);
IEMTermMatrix Dcc(Gamma, curlS(u_h), curlS(u_h), GF);
```

In the third example, we deal with lens-antenna design using a volume integral formulation of Maxwell equations.

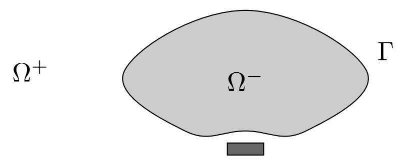

The subject has been widely considered in the physicist community but the mathematical results are not so numerous and most of them are very recent (e.g. [5], [6], [7]). With M. Costabel and E.-H. Koné, we investigated some mathematical results ([8]) and implemented the volume integral operators in MÉLINA++ with the contribution of D. Martin. The example involves the following integrands:

```
IEMTermMatrix IG(Omega, e_h, e_h, id(GF), "IdG");
```

$$\int_{\Omega^-}\int_{\Omega^-} \eta \boldsymbol{u}(y)\, G(x,y)\, dy\, \boldsymbol{v}(x)\, dx$$

and `IEMTermMatrix D2G(Omega, E_h, E_h, gradxgrady(GF), "D2G");`

$$\int_{\Omega^-} \boldsymbol{v}(x)\, \nabla_x \int_{\Omega^-} \eta \boldsymbol{u}(y) \cdot \nabla_y G(x,y)\, dy\, dx$$

Here `e_h` defines a scalar unknown and `E_h` defines a vectorial unknown. For lens-antenna design, alternatively, surface integral equation methods can be used which had been developed by F. Le Louër ([9]). This approach further reduces the number of unknowns and the numerical realization is considered together with C. Burkard and has been implemented in MÉLINA++.

References

[1] Available from **https://public.me.com/danielmartin** and from **http://anum-maths.univ-rennes1.fr/melina/**

[2] C. Hazard, M. Lenoir, *On the solution of time-harmonic scattering problems for Maxwell's equations*, SIAM J. Math. Anal. **27(6)** (1996), 1597–1630.

[3] F. Ben Belgacem, M. Fournié, N. Gmati, F. Jelassi, *On the Schwarz algorithms for the elliptic exterior boundary value problems*, ESAIM: M2AN **39(4)** (2005), 693–714.

[4] X. Antoine, M. Darbas, *Generalized combined field integral equations for the iterative solution of the Helmholtz equation in three dimensions*, M2AN **41(1)** (2007), 147–167.

[5] T. Hohage, *Fast numerical solution of the electromagnetic medium scattering problem and applications to the inverse problem*, J. Comp. Phys. **214** (2006), 224–238.

[6] A. Kirsch, *An integral equation approach and the interior transmission problem for Maxwell's equations*, Inverse Probl. Imaging **1(1)** (2007), 159–179.

[7] R. Potthast, *Electromagnetic scattering from an orthotropic medium*, J. Int. Eq. and Appl. **11** (1999), 179–215.

[8] M. Costabel, E. Darrigrand, E.H. Koné, *Volume and surface integral equations for electromagnetic scattering by a dielectric body*, J. Comput. Appl. Math. **234** (2010), 1817–1825.

[9] M. Costabel, F. Le Louër, *Shape derivatives of boundary integral operators in electromagnetic scattering*, HAL: hal-00453948 ; arXiv : 1002.1541v2.

Shape Reconstruction based on Integral Invariants: An Inverse Problem

Thomas Fidler

(joint work with Markus Grasmair and Otmar Scherzer)

In many applications, among them object recognition and shape optimisation, objects and shapes are involved and one faces the problem of describing the geometry of the object in a mathematical terminology. A common approach to tackle this problem is to use the well investigated framework of differential invariants. For instance, if one considers a two-dimensional object bounded by a sufficiently regular curve, the associated curvature function can be used to describe the object. In particular, features of the object like protrusions, corners or inflection points can be characterised by their curvature, and are, as a consequence, still present as features in the encoding. In addition, the curvature function is invariant with respect to rigid body motions applied to the object. However, since curvature, and also all other differential invariants, are based on differentiation, all of them are inherently sensitive to noisy data.

Integral invariants have been introduced by Manay et al. [6] as a tool for shape matching and classification. They enjoy similar invariance properties as their differential counterparts, but are more robust in the presence of noisy data. Apart from that, integral invariants still carry geometrical information about the object (cf. [1, 7]) and allow for a natural scale space of features, as they are capable to distinguish between features of small size and noise. Integral invariants have been used in many applications as a stable object encoding and, in addition, have proven to be successful for many tasks, among them object classification [4] and geometry processing [2], but also for segmentation with a prior [5].

In this talk we focus on two specific integral invariants — the cone and the circle area invariant —, which both have a simple geometrical interpretation as an intersection of the encoded object and a regular domain. We define the *circle area integral invariant* I^r_{circle} as the intersection of the object $\Omega \subset \mathbb{R}^n$ with a ball of radius $r > 0$ centred at the object's boundary $\partial\Omega$. More precisely,

$$I^r_{\text{Circle}}[\Omega](\boldsymbol{x}) := \mathcal{L}^n\big(\Omega \cap B_r(\boldsymbol{x})\big), \quad \boldsymbol{x} \in \partial\Omega.$$

The cone area integral invariant is introduced for a special class of objects that can be parametrised by a radial function. Let $\Omega_\gamma \subset \mathbb{R}^n$ be the *domain* generated by a non-negative continuous radial function γ mapping from $\mathbb{S}^{n-1}$ to the positive real numbers, i.e., for $\gamma > 0$ we define

$$\Omega_\gamma := \{t\boldsymbol{\tau} \in \mathbb{R}^n : 0 \leq t < \gamma(\boldsymbol{\tau}),\ \boldsymbol{\tau} \in \mathbb{S}^{n-1}\}.$$

The generated domain Ω_γ is open, star-shaped with respect to the point $\boldsymbol{x} = \boldsymbol{0}$, and its boundary curve has no self-intersections and admits a unique interior and exterior. We define the *cone area integral invariant* $I^\varepsilon_{\text{Cone}}$ as the intersection of such an object Ω_γ with a cone C_ε of aperture $\varepsilon > 0$ and apex equal to zero. More precisely,

$$I^\varepsilon_{\text{Cone}}(\boldsymbol{\sigma}) := \mathcal{L}^n\big(\Omega \cap C_\varepsilon(\boldsymbol{\sigma})\big), \quad \boldsymbol{\sigma} \in \mathbb{S}^{n-1},$$

where $C_\varepsilon(\boldsymbol{\sigma}) := \{t\boldsymbol{\tau} \in \mathbb{R}^n : \boldsymbol{\tau} \in \mathbb{S}^{n-1},\ \langle\boldsymbol{\tau},\boldsymbol{\sigma}\rangle \geq \cos(\varepsilon/2),\ t \geq 0\}$.

We briefly discuss the advantages of both integral invariants over other object encodings, as well as their limitations. In particular, we address the question whether the presented integral invariants are injective mappings allowing for a unique identification of an object with its invariant. In addition, we present some numerical results related to object recovery based on integral invariants. In particular, we investigate the ill-posed problem of reconstructing a star-shaped object from its Radon transform with only limited data available, and use the framework of integral invariants to stabilise the inversion. First, we rewrite the Radon transform of an object in terms of a generating radial function, which results in a non-linear operator. Then, we reformulate the ill-posed non-linear operator equation as a minimisation problem in terms of a Tikhonov like functional, where the penalty term is based on the difference of integral invariants. We show existence of minimisers and present a smooth approximation of the Tikhonov like functional for the numerical implementation. The advantages of this approach are discussed on the basis of the presented numerical results.

References

[1] T. Fidler, M. Grasmair, and O. Scherzer. Identifiability and reconstruction of shapes from integral invariants. *Inverse Probl. Imaging*, 2(3):341–354, 2008.

[2] Q.-X. Huang, S. Flöry, N. Gelfand, M. Hofer, and H. Pottmann. Reassembling fractured objects by geometric matching. In *ACM SIGGRAPH 2006 Papers*, SIGGRAPH '06, pages 569–578, New York, NY, USA, 2006. ACM.

[3] H. Krim and A. J. Yezzi, Jr. *Statistics and Analysis of Shapes*. Birkhäuser, Boston, 2006.

[4] S. Manay, D. Cremers, B.-W. Hong, A. J. Yezzi, Jr., and S. Soatto. Integral invariants and shape matching. In [3], pages 137–166, 2006.

[5] S. Manay, D. Cremers, A. J. Yezzi, Jr., and S. Soatto. One-shot integral invariant shape priors for variational segmentation. In Anand Rangarajan, Baba Vemuri, and Alan Yuille, editors, *Energy Minimization Methods in Computer Vision and Pattern Recognition*, volume 3757 of *Lecture Notes in Computer Science*, pages 414–426. Springer Berlin / Heidelberg, 2005.

[6] S. Manay, B.-W. Hong, A. J. Yezzi, Jr., and S. Soatto. Integral invariant signatures. In Toms Pajdla and Jir Matas, editors, *Computer Vision - ECCV 2004*, volume 3024 of *Lecture Notes in Computer Science*, pages 87–99. Springer Berlin / Heidelberg, 2004.

[7] H. Pottmann, J. Wallner, Q.-X. Huang, and Y.-L. Yang. Integral invariants for robust geometry processing. *Comput. Aided Geom. Design*, 26(1):37–60, 2009.

Shape Optimization for Free Boundary Problems

Helmut Harbrecht

(joint work with Karsten Eppler)

The present talk is dedicated to the solution of a generalized *Bernoulli exterior free boundary problem* which serves as a prototype for many shape optimization problems. Let $T \subset \mathbb{R}^n$ denote a bounded domain with *free boundary* $\partial T = \Gamma$. Inside the domain T we assume the existence of a simply connected subdomain $S \subset T$ with *fixed* boundary $\partial S = \Sigma$. The resulting annular domain $T \setminus \overline{S}$ is denoted by Ω.

The exterior free boundary problem under consideration might be formulated as follows: For given data f, g, h, seek the domain Ω and the associated function u such that the overdetermined boundary value problem

$$-\Delta u = f \text{ in } \Omega, \quad -\frac{\partial u}{\partial \mathbf{n}} = h, \; u = 0 \text{ on } \Gamma, \quad u = g \text{ on } \Sigma \tag{1}$$

is satisfied. Here, $g, h > 0$ and $f \geq 0$ are sufficiently smooth *functions* on $\mathbb{R}^n$ such that u provides enough regularity for a second order shape calculus. We like to stress that the positivity of the Dirichlet data implies that u is positive on Ω and thus it holds in fact $\partial u / \partial \mathbf{n} < 0$.

In order to numerically solve (1) by means of shape optimization we shall introduce two different state functions, namely

$$\begin{aligned} -\Delta v &= f \text{ in } \Omega, & v &= g \text{ on } \Sigma, & v &= 0 \text{ on } \Gamma, \\ -\Delta w &= f \text{ in } \Omega, & -\frac{\partial w}{\partial \mathbf{n}} &= h \text{ on } \Sigma, & w &= 0 \text{ on } \Gamma. \end{aligned} \tag{2}$$

Here, the state v solves the pure Dirichlet problem whereas the state w solves a mixed boundary value problem.

We will consider the following four formulations, where the infimum has always to be taken over all sufficiently smooth domains which include the domain S.

(i) An energy variational formulation is derived by using the Dirichlet energy. The solution $\big((\Omega, u(\Omega)\big)$ of (1) is the minimizer (cf. [3]) of the Dirichlet energy functional

$$J_1(\Omega) = \int_\Omega \big\{\|\nabla v\|^2 - 2fv + h^2\big\} d\mathbf{x} \to \inf. \tag{3}$$

(*ii*) A variational least-squares cost function, firstly proposed by Kohn and Vogelius [10] in the context of the inverse conductivity problem, is consider as second formulation:

$$J_2(\Omega) = \int_\Omega \|\nabla(v-w)\|^2 d\mathbf{x} = -\int_\Gamma v\left(h + \frac{\partial w}{\partial \mathbf{n}}\right) d\sigma \to \inf . \tag{4}$$

This functional seems to be very attractive since, due to

$$J_2(\Omega) \sim \|w\|_{H^{1/2}(\Gamma)} \left\| h + \frac{\partial v}{\partial \mathbf{n}} \right\|_{H^{-1/2}(\Gamma)},$$

the Dirichlet and Neumann data are both tracked in their natural trace spaces.

(*iii*) One can also consider the solution v of the pure Dirchlet problem and track the Neumann data in a least-squares sense relative to $L^2(\Gamma)$, that is

$$J_3(\Omega) = \frac{1}{2}\int_\Gamma \left(h + \frac{\partial v}{\partial \mathbf{n}}\right)^2 d\sigma \to \inf . \tag{5}$$

(*iv*) Correspondingly, if the Neumann datum h is assumed to be prescribed, the L^2-least square tracking of the Dirichlet boundary condition at Γ reads as

$$J_4(\Omega) = \frac{1}{2}\int_\Gamma w^2 d\sigma \to \inf . \tag{6}$$

Based on a shape calculus via boundary variations, developed in [1, 2], we computed the boundary integral representations of the shape gradients and Hessians of the four formulations in [3, 4, 5, 6], see also [8, 9]. With the shape Hessian at hand we are able to investigate the stability of the global minimizer $\Omega^\star$.

Due to the two-norm discrepency (see [7]), the shape Hessian defines a continuous bilinear form not in the strong Banach space X but in a weaker space $H^s(\Gamma) \supsetneq X$

$$d^2 J(\Omega) : H^s(\Gamma) \times H^s(\Gamma) \to \mathbb{R},$$

i.e., there holds the estimate

$$|d^2 J(\Omega)[dr_1, dr_2]| \le c_S \|dr_1\|_{H^s(\Gamma)} \|dr_2\|_{H^s(\Gamma)}.$$

This space is refered to as the *energy space* of the underlying functional. For the shape functionals (3)–(6) the energy spaces are $H^{1/2}(\Gamma)$ in case of J_1 and $H^1(\Gamma)$ in case of J_2, J_3, and J_4.

Accordingly, the second order Taylor remainder $R_2\big(J(\Omega), dr\big)$ satisfies

$$\big|R_2\big(J(\Omega), dr\big)\big| = o(\|dr\|_X)\|dr\|^2_{H^s(\Gamma)}.$$

Therefore, a local minimum $\Omega^\star$ is *stable* if the shape Hessian $d^2J(\Omega^\star)$ is strictly coercive in its energy space $H^s(\Gamma^\star)$

$$d^2 J(\Omega^\star)[dr, dr] \ge c_E \|dr\|^2_{H^s(\Gamma^\star)}, \quad c_E > 0.$$

functional	energy space	positivity space	posedness
J_1	$H^{1/2}$	$H^{1/2}$	well-posed
J_2	H^1	$H^{1/2}$	algebraically ill-posed
J_3	H^1	H^1	well-posed
J_4	H^1	L^2	algebraically ill-posed

Table 1. The energy spaces and the positivity spaces of the shape Hessians.

The shape problem under consideration is then *well-posed* and a nonlinear Ritz-Galerkin method produces approximate shapes that converge quasi-optimal with respect to the energy norm, see [7] for the details.

At the optimal domain, even though the shape gradients look quite different, the shape Hessians of the functionals (3)–(6) surprisingly consist of the same ingredients. Namely, in [3, 4, 5, 6], the following expressions have been proven for the shape Hessian at the optimal domain:

$$\begin{aligned}
d^2 J_1(\Omega^\star)[dr_1, dr_2] &= \big((\Lambda + \mathcal{A})\mathcal{M} dr_1, \mathcal{M} dr_2\big)_{L^2(\Gamma^\star)},\\
d^2 J_2(\Omega^\star)[dr_1, dr_2] &= \big((\Lambda + \mathcal{A})\mathcal{M} dr_1, \Lambda^{-1}(\Lambda + \mathcal{A})\mathcal{M} dr_2\big)_{L^2(\Gamma^\star)},\\
d^2 J_3(\Omega^\star)[dr_1, dr_2] &= \big((\Lambda + \mathcal{A})\mathcal{M} dr_1, (\Lambda + \mathcal{A})\mathcal{M} dr_2\big)_{L^2(\Gamma^\star)},\\
d^2 J_4(\Omega^\star)[dr_1, dr_2] &= \big(\Lambda^{-1}(\Lambda + \mathcal{A})\mathcal{M} dr_1, \Lambda^{-1}(\Lambda + \mathcal{A})\mathcal{M} dr_2\big)_{L^2(\Gamma^\star)},
\end{aligned}$$

where $\mathcal{M} : L^2(\Gamma^\star) \to L^2(\Gamma^\star)$ is a *bijective* multiplication operator, $\Lambda : H^{1/2}(\Gamma^\star) \to H^{-1/2}(\Gamma^\star)$ is the Dirichlet-to-Neumann map (associated with the pure Dirichlet problem in (2)) and

$$\mathcal{A} := \mathcal{H} + \left[\frac{\partial h}{\partial \mathbf{n}} - f\right] \Big/ g : L^2(\Gamma^\star) \to L^2(\Gamma^\star)$$

is a multiplication operator. Notice that $\Lambda^{-1} : H^{-1/2}(\Gamma^\star) \to H^{1/2}(\Gamma^\star)$ is the inverse of Λ, which has to be understood as the Neumann-to-Dirichlet map in the sense of the mixed boundary value problem in (2).

Consequently, in case of the functional J_1 and J_3 the positiveness is given with respect to the energy space $H^s(\Gamma^\star)$ which implies the well-posedness of these formulations of the free boundary problem. Whereas in case of the functionals J_2 and J_4 the positivity holds only in the weaker spaces $H^{1/2}(\Gamma^\star)$ and $L^2(\Gamma^\star)$, respectively, that is

$$d^2 J_2(\Omega^\star)[dr, dr] \geq c_E \|dr\|^2_{H^{1/2}(\Gamma^\star)}, \quad d^2 J_4(\Omega^\star)[dr, dr] \geq c_E \|dr\|^2_{L^2(\Gamma^\star)}, \quad c_E > 0.$$

This implies the algebraically *ill-posedness* of the underlying formulations. In particular, tracking the Dirichlet data in the L^2-norm is not sufficient. We strongly assume that they have to be tracked relative to H^1. Our results are summarized in Table 1.

References

[1] K. Eppler. Boundary integral representations of second derivatives in shape optimization. *Discuss. Math. Differ. Incl. Control Optim.* **20** (2000) 63–78.

[2] K. Eppler. Optimal shape design for elliptic equations via BIE-methods. *Appl. Math. Comput. Sci.* **10** (2000) 487–516.

[3] K. Eppler and H. Harbrecht. Efficient treatment of stationary free boundary problems. *Appl. Numer. Math.* **56** (2006) 1326–1339.

[4] K. Eppler and H. Harbrecht. Tracking Neumann data for stationary free boundary problems. *SIAM J. Control Optim.* **48** (2009) 2901–2916.

[5] K. Eppler and H. Harbrecht. Tracking the Dirichlet data in L^2 is an ill-posed problem. *J. Optim. Theory Appl.* **145** (2010) 17–35.

[6] K. Eppler and H. Harbrecht. On a Kohn-Vogelius like formulation of free boundary problems. *Comput. Optim. Appl.* (to appear).

[7] K. Eppler, H. Harbrecht, and R. Schneider. On convergence in elliptic shape optimization. *SIAM J. Control Optim.* **45** (2007) 61–83.

[8] J. Haslinger, K. Ito, T. Kozubek, K. Kunisch, and G. Peichl. On the shape derivative for problems of Bernoulli type. *Interfaces and Free Boundaries* **11** (2009) 317–330.

[9] K. Ito, K. Kunisch, and G. Peichl. Variational approach to shape derivatives for a class of Bernoulli problems. *J. Math. Anal. Appl.* **314** (2006) 126–149.

[10] R. Kohn and M. Vogelius. Determining conductivity by boundary measurements. *Comm. Pure Appl. Math.* **37** (1984) 289–298.

The Domain Derivative of Time-Harmonic Electromagnetic Waves at Interfaces

Frank Hettlich

In shape optimization as well as in inverse obstacle identification problems the domain derivative is a common approach. Usually based on integral representations or weak formulations of a boundary value problem it can be shown that there exists a derivative of functionals, which include the solution of the partial differential equation, with respect to variations of the underlying geometry (see for instance [4, 3, 7]). Additionally in view of further analytic and numerical investigations a representation of these derivatives again by a boundary value problem is of vital importance (see [2]).

In case of scalar valued functions for second order linear partial differential equations for many functionals and boundary conditions such representations are known. But in case of Maxwell's equation only a few results based on the integral equation approach are available (see [7, 5, 1]). The paper discusses the substantial problem for a weak approach to the domain derivative and succeeds in overcoming the difficulties.

We consider the scattering of electromagnetic waves at a domain given by different electric parameters. For the derivative with respect to variations of the interface, which is characterized by discontinuity of the coefficients of the Maxwell equations, we have to consider the difference of the solution of the perturbed and of the unperturbed boundary value problem. This requires a transformation of the field solving the perturbed problem such that the discontinuity occurs on the unperturbed boundary. But in case of Maxwell's equations such a change of variables in general leads to functions which are not in the natural Sobolev space, $H(\mathrm{curl}, \Omega)$ (see [6]). The loss of regularity causes the main problem in showing existence of the domain derivative for Maxwell's equations.

The paper presents a new idea which solves for this problem. Applying a curl invariant transformation to the electromagnetic field leads to functions in the correct function space. Thus instead of considering $E_h \circ \varphi$, where E_h is the electric field of the perturbed problem with diffeomorphism $\varphi(x) = x + h(x)$ and variation field h, we consider the transformed field $J_\varphi E_h \circ \varphi$, where J_φ denotes the Jacobian matrix of φ. After a change of variables this function is in $H(\mathrm{curl}, \Omega)$. Discontinuities of its traces only occur on the original boundary. Computing first order terms of the difference of these vector fields leads to a proof of existence of the so called material derivative for Maxwell's equations.

By splitting the material derivative into certain part we show next that outside a neighborhood of the discontinuities of coefficients the derivative can be represented by the domain derivative, which is a radiating solution of Maxwell's equations satisfying certain transmission boundary conditions at the interface. Still some work has to be done in extracting representations of these boundary conditions in such a way that the symmetric structure of the electric and the magnetic field can be observed and such that a numerical implementation of this boundary value problem can be achieved.

References

[1] M. Costabel, F. Le Louër, *Shape Derivatives of Boundary Integral Operators in Electromagnetic Scattering*, Preprint (2010).

[2] M. Ganesh, S.C. Hawkins *A high-order algorithm for multiple electromagnetic scattering in three Dimensions* Numer. Algorithms **50** (2009), 469–510.

[3] F. Hettlich, *Fréchet Derivatives in Inverse Obstacle Scattering,* Inverse Problems **11** (1995), 371–382.

[4] A. Kirsch, *The Domain Derivative and Two Applications in Inverse Scattering Theory* Inverse Problems **9** (1993), 81–96.

[5] R. Kress, *Electromagnetic waves scattering: Scattering by obstacles* In: Scattering (Pike, Sabatier, eds.), Academic Press, London (2001), 191–210.

[6] P. Monk *Finite element Methods for Maxwell's Equations*, Oxford University Press, 2003.

[7] R. Potthast, *Domain Derivatives in Electromagnetic Scattering*, Math. Meth. Appl. Sc. **19** (1996), 1157–1175.

Shape sensitivities for a two problems in lithotripsy

Barbara Kaltenbacher

Motivated by the application of high intensity focused ultrasound (HIFU) in lithotripsy, we consider two shape optimization problems, both being concerned with an optimal focusing of the ultrasound waves in order to concentrate the sound pressure peak to the kidney stones and avoid lesions of the surrounding tissue. They consist of optimizing the shape of

(a) a piezomosaic ("self-focusing") or

(b) an acoustic silicone lens.

The underlying model contains the equations of nonlinear acoustics, which are the Kuznetsov

$$\psi_{tt} - c^2\Delta\psi - b\Delta\psi_t = \left(\frac{1}{c^2}\frac{B}{2A}(\psi_t)^2 + |\nabla\psi|^2\right)_t \tag{1}$$

or the Westervelt

$$\psi_{tt} - c^2\Delta\psi - b\Delta\psi_t = \left(\frac{1}{c^2}(1+\frac{B}{2A})(\psi_t)^2\right)_t \tag{2}$$

equation, the latter being a simplification by neglecting local nonlinear effects (in the sense that the expression $c^2|\nabla\psi|^2 - (\psi_t)^2$ is sufficiently small). Here ϕ is the acoustic velocity potential, $c > 0$ is the speed of sound, $b \geq 0$ the diffusivity of sound, and B/A the parameter of nonlinearity. In case (b) we additionally have a coupling to the equation of elasticity within the lens via appropriate interface conditions (see below).

In order to compute shape gradients we make use of a general approach [2] which can be extended to the time dependent setting in a straightforward manner provided the cost function constains an integral over time: Consider minimization

$$\min J(U,\Omega,\Gamma) \equiv \int_0^T \Big(\int_\Omega j_1(U)\,dx + \int_\Gamma j_2(U)\,ds + \int_{\partial\Omega\setminus\Gamma} j_3(U)\,ds\Big)d\sigma$$

under a partial differential equation (PDE) constraint

$$\mathcal{E}(U,\Omega) = 0$$

where $\mathcal{E}(\cdot,\Omega) : \mathcal{V} \to \tilde{\mathcal{V}}^*$, $\mathcal{V},\tilde{\mathcal{V}}$ are Banach spaces, and $\tilde{\mathcal{V}}^*$ is the dual of $\tilde{\mathcal{V}}$. The manifold Γ to be optimized is supposed to be the boundary $\Gamma = \partial\mathcal{D}$ of some domain $\mathcal{D}$ being contained in a hold-all $\mathcal{U} \subseteq \mathbb{R}^d$ such that $\overline{D} \subseteq \mathcal{U}$, and for the domain Ω where the PDE is supposed to hold there are three possible cases:

$$(i)\ \Omega = \mathcal{D} \ \text{ or } (ii)\ \Omega = \mathcal{U} \ \text{ or } (iii)\ \Omega = \mathcal{U}\setminus\mathcal{D}\,;$$

The domain transformations are carried out via families of mappings $\{F_\tau \,|\, \tau \in (-\tau_0,\tau_0)\}$ as follows:

$$F_\tau : \mathcal{U} \to \mathbb{R}^d\,, \quad F_\tau = \mathrm{id} + \tau h\,, \quad \Omega_\tau = F_\tau(\Omega)\,, \quad \Gamma_\tau = F_\tau(\Gamma)$$

where the vector field $h \in C^{1,1}(\mathcal{U},\mathbb{R}^d)$, $h|_{\partial\mathcal{U}} = 0$.

Applying extension of the result on the Eulerian derivative
$dJ(U,\Omega,\Gamma) = \lim_{\tau\to 0}\frac{1}{\tau}(J(U_\tau,\Omega_\tau,\Gamma_\tau) - J(U,\Omega,\Gamma))$ from [2] first of all to the shape optimization (a), we consider the setting $\Omega = \Omega_f = \mathcal{U}\setminus\mathcal{D}$, $\Gamma = \Gamma_{Neum}$ $U = \psi$

$$j_1(U,\Omega) = |\rho_f\psi_t - y^d|^2\,,\ j_2 = 0\,,\ j_3 = 0\,, \tag{3}$$

(note that $\rho_f\psi_t$ is the acoustic pressure and y^d is the desired acoustic pressure), $\mathcal{E}(U,\Omega)$ corresponds to the Westervelt equation (2) in the fluid region Ω_f with $\partial\Omega = \Gamma_{abs} \cup \Gamma_{Neum}$, absorbing boundary conditions $\frac{1}{c}\psi_t + \frac{\partial\psi}{\partial n} = 0$ on Γ_{abs}, boundary excitation $\frac{\partial\psi}{\partial n} = 0$ on Γ_{Neum}, as well as homogeneous initial conditions: $\psi(0) = \psi_t(0) = 0$.

The strong form of the adoint PDE reads as

$$\begin{aligned}
&(1-2k\psi_t)p_t)_t - c^2\Delta p + b\Delta p_t = j_{1,\psi}(U) \quad \text{in } (0,T)\times\Omega_f \\
&\tfrac{1}{c}p_t - \tfrac{\partial p}{\partial n} = 0 \quad \text{on } (0,T)\times\Gamma_{abs} \\
&\tfrac{\partial p}{\partial n} = 0 \quad \text{on } (0,T)\times\Gamma_{Neum}
\end{aligned}$$

with the end conditions

$$\vec{p}(T) = 0\,,\ \vec{p}_t(T) = 0 \text{ in } \Omega_s \quad p(T) = 0\,,\ p_t(T) = 0 \text{ in } \Omega_f\,,$$

and the additional initial boundary conditions (due to the strong damping term with coefficient $b > 0$) $p(0) = 0$ on Γ_{abs}. Therewith, formally we arrive at the following expession for the shape gradient

$$\begin{aligned}
dJ(U,\Omega) \;=\; \int_{\Gamma_{Neum}}\int_0^T \Big\{ & -(1-k\psi_t)\psi_t p_t + (c^2\nabla\psi + b\nabla\psi_t)\nabla p \\
& + j_1(\psi) + \frac{\partial(c^2 g + b g_t)p}{\partial n} + \kappa(c^2 g + b g_t)p \Big\} h^T n\, d\sigma\, ds
\end{aligned}$$

Verification of the (time integrated) assumptions from [2] is expected to be doable by combining techniques from [2], [3], [1].

We mention in passing that an advantageous formulation might be obtained via the alternative setting $\Omega = \Omega_f = \mathcal{U}\setminus\mathcal{D}$ by putting h to zero on the absorbing boundary.

To deal with the shape optimization problem (b) in the framework of the extension of [2], we set $\Omega = \mathcal{U} = \Omega_f \cup \Omega_s$, $\mathcal{D} = \Omega_s$, $\Gamma = \Gamma_i$, $U = (\vec{u},\psi)$ (3), and $\mathcal{E}(U,\Omega)$ corresponds to the Westervelt equation (2) in the fluid region Ω_f, together with the equation of linear elasticity in the solid region Ω_s:

$$\rho_s \vec{u}_{tt} - \mathcal{B}^T(\underline{c}\mathcal{B}\vec{u}) = 0$$

via interface conditions on Γ_i:

$$\begin{aligned}
&\vec{u}_t \cdot n_s = \tfrac{\partial\psi}{\partial n_f} \quad \text{(continuity of normal velocity)} \\
&\underline{\sigma} n_s = \rho_f \psi_t n_f \quad \text{(surface force acts as pressure load)}\,,
\end{aligned}$$

absorbing boundary conditions on Γ_{abs}, Neumann boundary excitation on Γ_{Neum}, and homogeneous initial conditions. This time, the strong form of the adjoint problem is as follows:

$$\begin{aligned}
&\rho_s \vec{p}_{tt} - \mathcal{B}^T \underline{c}^T \mathcal{B}\vec{p} = 0 \quad \text{in } (0,T)\times\Omega_s \\
&(1-2k\psi_t)p_t)_t - c^2\Delta p + b\Delta p_t = j_{1,\psi}(U) \quad \text{in } (0,T)\times\Omega_f \\
&\tfrac{1}{c}p_t - \tfrac{\partial p}{\partial n} = 0 \quad \text{on } (0,T)\times\Gamma_{abs} \\
&\tfrac{\partial p}{\partial n} = 0 \quad \text{on } (0,T)\times\Gamma_{Neum} \\
&\vec{u}\cdot n_s = \tfrac{\partial\tilde{\psi}}{\partial n_f} \quad \text{on } (0,T)\times\Gamma_i \qquad \text{where } \underline{\tilde{\sigma}} = (\underline{c}^T\mathcal{B}\vec{p}) \\
&\underline{\tilde{\sigma}} n_s = \rho_f \tilde{\psi}_t n_f \quad \text{on } (0,T)\times\Gamma_i \qquad \text{and } \tilde{\psi} = \frac{1}{\rho_f}(c^2 p - b p_t)
\end{aligned}$$

with the end conditions

$$\vec{p}(T) = 0\,,\ \vec{p}_t(T) = 0 \text{ in } \Omega_s \quad p(T) = 0\,,\ p_t(T) = 0 \text{ in } \Omega_f\,,$$

and the additional initial boundary conditions $p(0) = 0$ on Γ_i , $p(0) = 0$ on Γ_{abs} .

Therewith, the shape gradient can be formally derived to be

$$\begin{aligned} dJ(U,\Omega) \;=\; & \int_{\Gamma_i}\int_0^T \Big\{ \Big(\rho_s(\vec{u}_t)^T \vec{p}_t - (\mathcal{B}\vec{u})^T \underline{c}(\mathcal{B}\vec{p}) \\ & -(1-k\psi_t)\psi_t p_t + (c^2\nabla\psi + b\nabla\psi_t)\nabla p \\ & -\tfrac{\partial \rho_f \psi_t \vec{p}^T n}{\partial n} - \kappa\rho_f\psi_t\vec{p}^T n + \tfrac{\partial (c^2\vec{u}_t + b\vec{u}_{tt})^T np}{\partial n} + \kappa(c^2\vec{u}_t + b\vec{u}_{tt})^T np \\ & -j_1|_{\Omega_f}(U) \Big\} h^T n \, d\sigma \, ds\,. \end{aligned}$$

Again, the assumptions from [2] can probably be verified, provided we have well-posedness of the coupled elastic-nonlinearly acoustic system. The latter is an still an open problem and subject of ongoing research, though.

Acknowledgment We wish to thank Gunter Peichl for fruitful discussions on [2] in the context of the applications considered here.

References

[1] C. Clason, B.Kaltenbacher, S. Veljovic, Boundary optimal control of the Westervelt and the Kuznetsov equation, *JMAA*, vo 356, pp 738-751, 2009.

[2] K.Ito, K.Kunisch, and G. Peichl, *Variational approach to shape derivatives*, ESAIM: COCV, **14** (2008), 517–539.

[3] B. Kaltenbacher and I. Lasiecka, *Global existence and exponential decay rates for the Westervelt equation*, Discrete and Continuous Dynamical Systems Series S, vol 2, pp. 503-525, 2009.

The Factorization Method for a Conductive Boundary Condition

Andreas Kirsch

(joint work with Andreas Kleefeld)

In this talk we consider a simple inverse scattering problem for the Helmholtz equation $\Delta u + k^2 u = 0$ in $\mathbb{R}^3$ where the scattering object consists of a bounded domain D covered by a thin layer of high conductivity. Mathematically, this leads to a transmission problem with a conductive transmission condition

$$u_+ \;-\; u_- \;=\; 0 \text{ on } \partial D \quad \text{and} \quad \frac{\partial u_+}{\partial \nu} \;-\; \frac{\partial u_-}{\partial \nu} \;+\; i\,\lambda\, u \;=\; 0 \text{ on } \partial D\,,$$

where $\pm$ denotes the limit from the exterior or interior of D, respectively. We show briefly how to apply the boundary integral equation method for treating the direct problem analytically and numerically by a collocation method. Then we study the inverse problem to determine the shape of the domain from the far field operator $F : L^2(S^2) \to L^2(S^2)$, defined by

$$(Fp)(\hat{x}) \;=\; \int_{S^2} p(\hat{\theta})\, u^\infty(\hat{x};\hat{\theta})\, \mathrm{d}s(\hat{\theta})\,, \quad \hat{x} \in S^2\,.$$

Here, $u^\infty(\hat{x};\hat{\theta})$ denotes the far field pattern of the scattered field at observation direction $\hat{x}$ and direction $\hat{\theta}$ of the incident plane wave. We use the Factorization method to express the characteristic function of the domain by a series which can easily computed from the scattering data.

We consider two cases. In the first case all of the boundary is covered by the layer; that is, $\lambda > 0$ on all of ∂D. Then we can prove that a given point $z \in \mathbb{R}^3$ belongs to D if, and only if, the series

$$(*) \qquad \sum_{j\in\mathbb{N}} \frac{|\langle \phi_z, \psi_j \rangle_{L^2(S^2)}|^2}{\lambda_j}$$

converges. Here, $\phi_z(\hat{x}) = \exp(-ik\, z\cdot\hat{x})$, and $\{\lambda_j, \psi_j : j \in \mathbb{N}\}$ is an orthonormal eigen system of the compact and positive operator $\operatorname{Im} F = (F - F^*)/(2i)$ which is known from the data.

In the second case the boundary is only partially covered by the layer; that is, the function λ vanishes on a part of ∂D. Then the scattering problem reduces to a scattering problem for an open surface, and we have to test the space with small surfaces $S \subset \mathbb{R}^3$ rather than points $z \in \mathbb{R}^3$. Then we show that the test surface S belongs to ∂D if, and only if the series $(*)$ converges where now ϕ_z is replaced by the single layer on S with constant density.

Some three-dimensional numerical experiments demonstrate the usefullness of the method.

Newton Regularizations for EIT: The Complete Electrode Model and Convergence by Local Injectivity

Armin Lechleiter
(joint work with Andreas Rieder)

The impedance tomography problem is certainly among the most important inverse problems, inspiring both important theoretical identification results and powerful computational techniques, see, e.g., [1] for an overview. Among the classical numerical methods for this ill-posed and non-linear problem are Newton-type methods based on local linearization. However, there exist few theoretical convergence results for such methods. In [3] we considered the complete electrode model of impedance tomography and proved that the Fréchet derivative of the underlying non-linear forward operator (mapping the conductivity to the current-to-voltage map) is, under suitable assumptions, injective. Since the complete electrode model is intrinsically finite-dimensional this implies that the forward operator satisfies a non-linearity condition that allows to prove convergence results for (inexact) Newton schemes applied to the inverse problem.

1. Impedance Tomography and the Complete Electrode Model

The impedance tomography problem is to reconstruct a conductivity $\gamma \in L^\infty(B)$ in some Lipschitz domain $B \subset \mathbb{R}^2$ from boundary measurements. For the complete electrode model these measurements are given by a finite-dimensional linear operator. We assume that γ is strictly bounded from below away from zero, and we introduce $p \in \mathbb{N}$ disjoint, open, and non-empty electrodes $E_1, \dots, E_p \subset \partial B$. See Figure 1(a) for a sketch. Denote by $\chi_{E_1}, \dots, \chi_{E_p}$ the indicator functions of the electrodes and by

$$\mathcal{E}_p = \operatorname{span}\{\chi_{E_j},\, j = 1, \dots, p\} \cap L^2_\diamond(\partial B)$$

the space of piecewise constant functions that vanish on the gaps in between the electrodes, and that additionally belong to $L^2_\diamond(\partial B) = \{f \in L^2(\partial B), \int_{\partial B} f \,\mathrm{d}s = 0\}$. The current-to-voltage map $\Lambda_p : \mathcal{E}_p \to \mathcal{E}_p$ maps a current I to the electrode voltages U, part of the solution $(u, U) \in H^1(B) \oplus \mathcal{E}_p$ of the problem

$$\begin{aligned}
&\nabla \cdot (\gamma \nabla u) = 0 \quad \text{in } B, \\
&u + z_j (\gamma \nabla u).\nu = U \quad \text{on } \cup_{j=1}^p E_j, \\
&(\gamma \nabla u).\nu = 0 \quad \text{on } \partial B \setminus \cup_{j=1}^p \overline{E_j}, \\
&\int_{E_j} (\gamma \nabla u).\nu \,\mathrm{d}s = I|_{E_j} \quad \text{for } j = 1, \dots, p.
\end{aligned} \tag{1}$$

The latter complete electrode model is a standard model for impedance tomography in the context of medical applications, compare [6]. Obviously, since the current-to-voltage map Λ_p is a linear operator between finite-dimensional spaces, it is impossible to reconstruct conductivities γ in infinite-dimensional function spaces. Hence, we propose to restrict ourselves to $\gamma \in V_{\mathcal{T}}^+$, the restrictions to B of piecewise polynomial functions on a mesh $\mathcal{T}$ of some domain D containing Ω. See Figure 1(b) for a sketch of B, D, and the mesh $\mathcal{T}$. Additionally, functions in $V_{\mathcal{T}}^+$ need to be bounded from below away from zero by some constant $c > 0$.

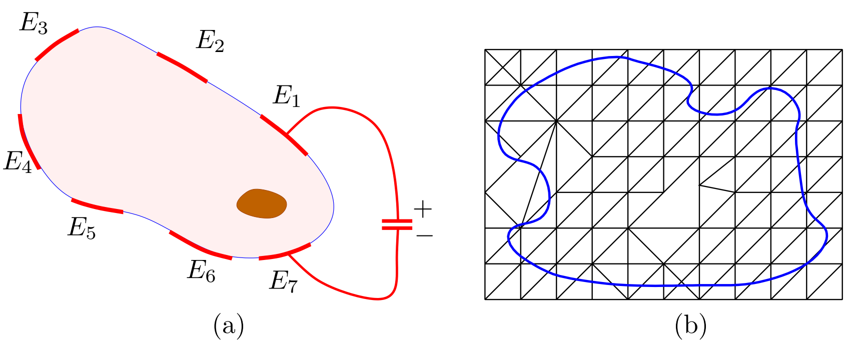

Figure 1. (a) Electrodes attached to the boundary of a conducting object under investigation. (b) The domain B (blue curve) is contained in a (rectangular) domain D with triangulation $\mathcal{T}$.

2. Main Results

Our main results show that if the electrodes on the boundary of B are sufficiently "dense", then the Fréchet derivative of F_p mapping $\gamma \in V_{\mathcal{T}}^{+}$ to Λ_p is injective, see Theorem 4.3 in [3]. This result is asymptotic: We consider a sequence of electrode configurations $\{E_j^p\}_{j=1}^p$ for $p \in \mathbb{N}$ where the pth configuration consists of p electrodes. For each electrode configuration we associate the configurations of the gaps $\{G_j^p\}_{j=1}^p$ in between the electrodes. We moreover need to assume that $\lim_{p\to\infty} \sum_{j=1}^p |G_j^p|^\theta = 0$ for some $\theta \in (0,1)$. Under these assumptions, the statement of [3, Theorem 4.3] is that for p large enough the Fréchet derivative of F_p is injective. An important ingredient of the proof are the localized potentials from [2].

Using this result, Theorem 5.4 in [3] establishes that F_p satisfies the so-called tangential cone condition. This condition in turn implies a convergence and regularization theory for inexact Newton schemes applied to the equation $F_p(\gamma) = \Lambda_p$, compare [4]. Note that all the above results carry over to the fully-discrete case where the variational formulation corresponding to problem (1) is discrete using finite elements with a sufficiently small mesh width.

References

[1] A. Adler, R. Gaburro, and W. Lionheart, EIT, in: Handbook of Mathematical Methods in Imaging, Springer, 2010.
[2] B. Gebauer, *Localized potentials in electrical impedance tomography*, Inverse Problems and Imaging **2** (2008), 251–269.
[3] A. Lechleiter and A. Rieder, *Newton regularizations for impedance tomography: convergence by local injectivity*, Inverse Problems **24** (2008), 065009.
[4] A. Rieder, Keine Probleme mit Inversen Problemen, Vieweg, 2003.
[5] O. Scherzer, *The use of Morozov's discrepancy principle for Tikhonov regularization for solving nonlinear ill-posed problems*, Computing **51** (1993), 45–60.
[6] E. Somersalo, M. Cheney and D. Isaacson, *Existence and Uniqueness for Electrode Models for Electric Current Computed Tomography*, SIAM J. Appl. Math. **52** (1992), 1023–1040.

Regularized Newton methods for electromagnetic inverse obstacle scattering problems

Frédérique Le Louër
(joint work with Thorsten Hohage)

We analyze the inverse problem to reconstruct the shape of a three dimensional perfectly conducting obstacle from electromagnetic noisy far field measurements.

Let Ω denote a bounded domain in $\mathbb{R}^3$ and let Ω^c denote the exterior domain $\mathbb{R}^3 \backslash \overline{\Omega}$. We assume that the boundary Γ of Ω is a simply connected closed surface, so that Ω is diffeomorphic to a ball. The outer unit normal vector on the boundary Γ is denoted by $\boldsymbol{n}$. Consider the perfect conductor problem : Given an incident electric wave $\mathbf{E}^{inc} \in \boldsymbol{H}_{loc}(\mathbf{curl}, \mathbb{R}^3)$ that satisfies $\mathbf{curl}\,\mathbf{curl}\,\mathbf{E}^{inc} - \kappa_e^2 \mathbf{E}^{inc} = 0$ in a neighborhood of $\overline{\Omega}$, find the electric scattered wave $\mathbf{E}^s \in \boldsymbol{H}_{loc}(\mathbf{curl}, \overline{\Omega^c})$ which solves :

$$\mathbf{curl}\,\mathbf{curl}\,\mathbf{E}^s - \kappa^2 \mathbf{E}^s = 0 \quad \text{in } \Omega^c, \tag{1}$$

$$\boldsymbol{n} \times (\mathbf{E}^s + \mathbf{E}^{inc}) = 0 \quad \text{on } \Gamma, \tag{2}$$

$$\lim_{|x| \to +\infty} |x| \left| \mathbf{curl}\,\mathbf{E}^s(x) \times \frac{x}{|x|} - i\kappa \mathbf{E}^s(x) \right| = 0. \tag{3}$$

It is well known that the above boundary value problem admits a unique solution for any positive real values of the exterior wave number κ (see [7] for a proof via boundary integral equation method). The radiation condition implies that the solution has an asymptotic behavior of the form

$$\mathbf{E}^s(x) = \frac{e^{i\kappa|x|}}{|x|} \mathbf{E}^\infty(\hat{x}) + O\left(\frac{1}{|x|}\right), \quad |x| \to \infty,$$

uniformly in all directions $\hat{x} = \dfrac{x}{|x|}$. The far field $\mathbf{E}^\infty$ is defined on the unit sphere S^2 and $\mathbf{E}^\infty \in \boldsymbol{L}^2_t(S^2) = \{\boldsymbol{h} \in \boldsymbol{L}^2(S^2);\ \boldsymbol{h}(\hat{x}) \cdot \hat{x} = 0\}$.

For a fixed incident plave wave $\mathbf{E}^{inc} = \vec{p}\, e^{i\kappa x \cdot d}$ with $\vec{p} \cdot d = 0$ and a fixed wavenumber κ, we consider the boundary to far field operator

$$F : \Gamma \mapsto \mathbf{E}^\infty \in \boldsymbol{L}^2_t(S^2)$$

which maps the boundary of the scatterer Ω onto the far field pattern $\mathbf{E}^\infty$ of the scattered field $\mathbf{E}^s$. The inverse problem of interest is : Given noisy far field data $\mathbf{E}^\infty_{*,\delta}$ obtained from the scattering of one or several incident plane waves, solve

$$F(\Gamma) = \mathbf{E}^\infty_{*,\delta}.$$

Although such an inverse problem is theoretically difficult to solve since it is ill-posed and nonlinear, one can apply numerical methods to recover an approximate solution. The use of regularized iterative scheme to solve numerically this equation require the study of the dependence of the operator F on the shape of the boundary of the scatterer. To this end, as usual, we choose a fixed reference domain Ω_{ref} with boundary Γ_{ref} and we consider variations generated by transformations of the form $x \mapsto x + r(x)$ of point x in the space $\mathbb{R}^3$. The functions r are assumed to be sufficiently small elements of the Banach space $\mathscr{C}^2(\Gamma, \mathbb{R}^3)$ in order that $(\mathrm{I} + r)$ is a diffeomorphism from Γ_{ref} to $\Gamma_r = (\mathrm{I} + r)\Gamma_{ref} = \{x + r(x);\ x \in \Gamma_{ref}\}$, so that the surface Γ_r is the boundary of a domain Ω_r diffeomorphic to the unit ball of $\mathbb{R}^3$. We define the set of admissible variations

$$\mathcal{V}_{ad} = \{r \in \mathscr{C}^2(\Gamma_{ref}, \mathbb{R}^3);\ \Gamma_r \text{ is diffeomorphic to } S^2\}.$$

The mapping $\mathcal{F} : r \in \mathcal{V}_{ad} \mapsto F(\Gamma_r) \in \boldsymbol{L}^2_t(S^2)$ is well defined. We distinguish the quantities related to the exterior Dirichlet scattering problem for the domain Ω_r through the subscript r. The following theorem is a rewriting, for the electric field only, of the characterization established in [6] by Kress and in [8] by Potthast.

Theorem. *The mapping* $\mathcal{F} : \mathcal{V}_{ad} \to \boldsymbol{L}_t^2(S^2)$ *is Fréchet differentiable with the Fréchet derivative at* r *in the direction* $\xi \in \mathscr{C}^2(\Gamma_{ref}, \mathbb{R}^3)$ *given by*

$$\mathcal{F}'[r]\xi = \mathbf{E}^{\infty}_{r,\xi},$$

where $\mathbf{E}^{\infty}_{r,\xi}$ *is the far field of the solution* $\mathbf{E}^{s}_{r,\xi}$ *to the Maxwell equation* (1) *in* Ω_r^c *that satisfies the Silver-Müller radiation condition and the Dirichlet boundary condition*

$$\begin{aligned}\boldsymbol{n}_r \times \mathbf{E}^{s}_{r,\xi} = &- \left(\xi\circ(\mathrm{I}+r)^{-1} \cdot \boldsymbol{n}_r\right) \left(\boldsymbol{n}_r \times \mathbf{curl}(\mathbf{E}^s_r + \mathbf{E}^{inc})\right) \times \boldsymbol{n}_r \\ &+ \frac{1}{\kappa^2}\,\mathbf{curl}_{\Gamma_r}\left(\left(\xi\circ(\mathrm{I}+r)^{-1} \cdot \boldsymbol{n}_r\right) \mathrm{curl}_{\Gamma_r}\left(\left(\boldsymbol{n}_r \times \mathbf{curl}(\mathbf{E}^s_r + \mathbf{E}^{inc})\right) \times \boldsymbol{n}_r\right)\right).\end{aligned}$$

on Γ_r *where* $\mathbf{E}^s_r$ *is the solution of the scattering problem* (1)-(3) *satisfying the Dirichlet boundary condition*

$$\boldsymbol{n}_r \times \left(\mathbf{E}^s_r + \mathbf{E}^{inc}\right) = 0 \quad \text{on } \Gamma_r.$$

(We refer to [7] *for the definition of the tangential vector curl* $\mathbf{curl}_\Gamma$ *and surface scalar curl* curl_Γ*).*

We can then apply the *iteratively regularized Gauss-Newton method* to the equation $\mathcal{F}'[r]^*\mathcal{F}'[r]\xi = \mathcal{F}'[r]^*\left(\mathbf{E}^{\infty}_{*,\delta} - \mathcal{F}[r]\right)$ (see [1, 3, 4]). We start with an initial guess r_0^δ and we update : $r^\delta_{n+1} = r^\delta_n + \xi^\delta_n$ where ξ^δ_n solves

$$\xi^\delta_n := \underset{\xi}{\operatorname{argmin}} \;\; ||\mathcal{F}'[r^\delta_n]\xi + F[r^\delta_n] - \mathbf{E}^{\infty}_{*,\delta}||_{\boldsymbol{L}^2(S^2)} + \alpha_n||\xi + r^\delta_n - r_0||$$

and is given by

$$\xi^\delta_n = \left(\alpha_n \mathrm{I} + \mathcal{F}'[r^\delta_n]^*\mathcal{F}'[r^\delta_n]\right)^{-1}\left(\mathcal{F}'[r^\delta_n]^*\left(\mathbf{E}^{\infty}_{*,\delta} - \mathcal{F}[r^\delta_n]\right) + \alpha_n\left(r_0 - r^\delta_n\right)\right).$$

We compute numerically ξ_n by applying the CGNE method and the regularization parameters α_n are chosen of the form $\alpha_n = \alpha_0 \cdot \gamma^n$ with $0 < \gamma < 1$ (see [4]). At each iteration the far field $\mathcal{F}[r]$ and the Fréchet derivative $\mathcal{F}[r]'\xi$ are computed with the help of two different boundary integral equation methods via the spectral algorithm of Ganesh and Graham [2] which ensures superalgebraic convergence. The library developped by Ivanyshyn [5] and based on MATLAB programming code which enables the numerical resolution and the graphical representation of three dimensional acoustic inverse obstacle scattering problems was used.

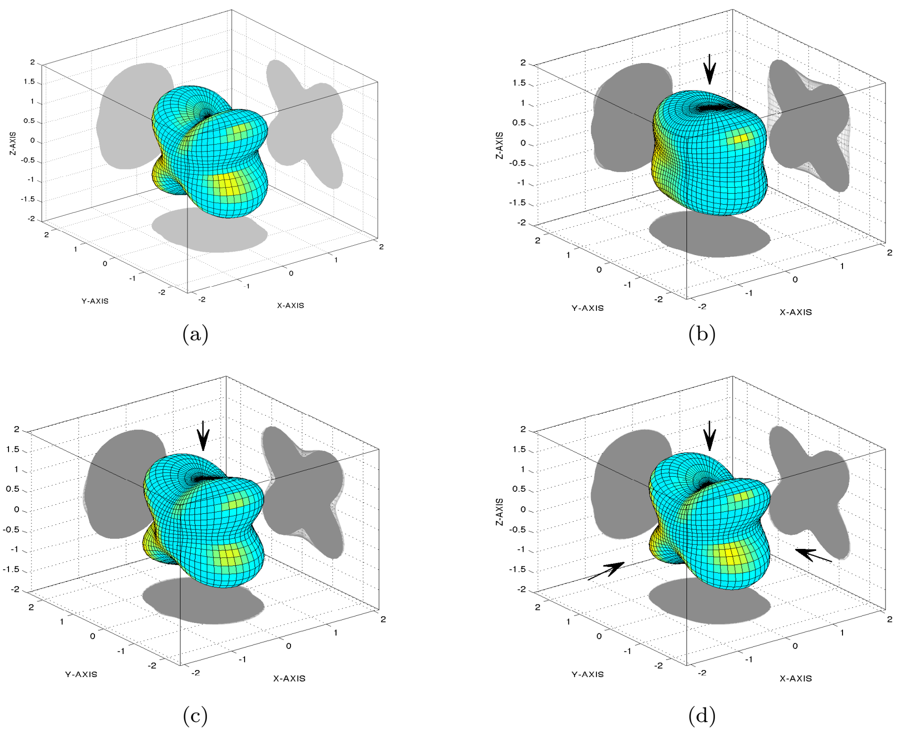

(a) original shape; reconstruction obtained at iteration 10 (b) with 1 incident plane wave, 1% noise, $\varnothing \sim \frac{\lambda}{2}$, (c) with 1 incident plane wave, 1% noise, $\varnothing \sim \lambda$ and (d) with 3 incident plane waves, 5% noise, $\varnothing \sim \lambda$, starting from the unit sphere as an initial guess.

References

[1] A. B. Bakushinskiĭ, *On a convergence problem of the iterative-regularized Gauss-Newton method*, Comput. Math. Math. Phys, **32** (1992), 1503–1509.

[2] M. Ganesh and I. G. Graham, *A high-order algorithm for obstacle scattering in three dimensions*, J. Comput. Phys., **198** (2004), 211–242.

[3] H. Harbrecht and T. Hohage, *Fast methods for three-dimensional inverse obstacle scattering problems*, J. Integral Equations Appl., **19** (2007), 237–260.

[4] T. Hohage, *Iterative Methods in Inverse Obstacle Scattering: Regularization Theory of Linear and Nonlinear Exponentially Ill-Posed Problems*, PhD in Numerical analysis, University of Linz, 1999.

[5] O. Ivanyshyn and R. Kress , *Identification of sound-soft 3D obstacles from phaseless data*, Inverse Probl. Imaging, **4** (2010), 1, 131–149.

[6] R. Kress, *Electromagnetic waves scattering : Scattering by obstacles*, Scattering, (2001), 191–210. Pike, E. R. and Sabatier, P. C., eds., Academic Press, London.

[7] J.-C. Nédélec, *Acoustic and electromagnetic equations*, vol. 144 of Applied Mathematical Sciences, Springer-Verlag, New York, 2001. Integral representations for harmonic problems.

[8] R. Potthast, *Domain derivatives in electromagnetic scattering*, Math. Methods Appl. Sci., **19** (1996), 15, 1157–1175.

Inverse spectral problem for identifying damage in steel concrete composite beam; Active thermography and the dynamical probe method

Gen Nakamura

The content of the talk consisted of two parts. The one was on the damage detection of a steel and concrete composite beam which is a fundamental unit of usual bridges of span of 60 to 80 meters long using 3 to 5 eigenvalues and the transversal components of the corresponding eigenfunctions. Usually a typical damage occurs in the connectors which connect the steel beam and concrete beam. This can be described as a decrease in the value of axial stiffness μ and shear stiffness k of the governing system of equations which models the deformation of the composite beam.. The scheme to identify the damage is the least square method. The minimization of the least square functional was done by using the projected conjugate gradient method. Due to the self-adjoint nature of the initial and boundary value problem for the governing system, by assuming that the eigenvalues are all simple, which is really the case we have for real measurements, we could compute the Frechet derivatives with respect to μ and k of the least square functional. We had a very good recovery of μ and k for synthetic data even if there are some noise. But recovery of μ is much better than k. This can be understood, because the transversal components of eigenfunctions give a good control on μ. For the experimental data we have when there is one single damage in the right end connector of the composite beam in different damage stages. They are stage I to stage IV, which are 25%, 40%, 70% and 100% cut of the connector, respectively. We obtained a practically acceptable recovery for μ, while the recovered k had some oscillation. Looking at the modulus of the derivative of the least square functional, we noticed that the modulus of the partial derivative with respect to μ becomes zero at 61 step of iteration of the projected gradient method. However even at this step the derivative of the least square function with respect to k is not zero and it started to grow as we proceed further steps. This study would be the first attempt to apply the variations of eigenvalues and eigenfunctions to an inverse problem with finite eigen-data. The same kind of argument can be applied to detect unknown boundaries such as cracks, cavities and inclusions from finite eigen-data. Overall the results show that the proposed scheme is already practically effective but it needs further study to improve the results. The second part of the talk was devoted to a mathematical analysis for the active thermography which could be its mathematical foundation. The active thermography is a non-destructive testing which is to detect unknown cracks, cavities and inclusions inside a heat conductor by injective heat fluxes by a flush lamp or heater and measuring the corresponding temperature distributions on the boundary of the conductor by a infrared camera. This measurement is a non-contact and very fast measurement, and the resolution of measuring the temperature distribution is 0.02 K. If there is a cooling part at some part of the boundary, the temperature distribution inside the conductor decays exponentially to 0 after switching off injecting heat flux. So, we can repeat the measurement many times and we can even superposed the measured data. As a mathematical idealization of this data acquisition, we took the so called Neumann to Dirichlet map as our measured data. We gave the scheme called dynamical probe method to identify for instance unknown separated inclusions inside the conductors from the Neumann to Dirichlet map. The scheme is mathematically rigorous. The ingredients of the schemes are the fundamental solutions, Runges approximation, reflected solution and indicator function. It is an open problem to identify unknown non-separated inclusions. The scheme has to be tested with real data. For that what kind of injected heat flux is available and how robust the scheme is would be major problems.

References

[1] S. Jimbo, A. Morassi, G. Nakamura and K. Shirota, *A Non Destructive Method for Damage Detection in Steel-Concrete Structures Based on Finite Eigendata*, submitted to Inverse Problems in Science and Engineering (2010).

[2] V. Isakov, K. Kim and G. Nakamura, *Reconstruction of an unknown inclusion by thermography*, Vol. IX, issue 4 (2010) pp. 34.

Mathematics and Application of Data Assimilation Algorithms

Roland W.E. Potthast

We survey approaches to solve atmospherical data assimilation problems and raise basic analytical questions to investigate the convergence analysis of data assimilation (DA) algorithms.

Data assimilation uses a large variety of measurements to determine the current state of some dynamical system, for atmospherical problems that is the current state of the Atmosphere. Data include in-situ measurements, data from moving devices (like planes) and remote sensing data from ground stations, planes and satellites. There are variational approaches as 3dVar, 4dVar and various versions of stochastical filters. We describe the key convergence questions and put them into a framework usually used to study iterative algorithms for inverse problems. For example, the standard update formula for 3dVar or the Kalman Filter, respectively, is given by

$$\varphi^{(a)} = \varphi^{(b)} + (\alpha I + A^* A)^{-1} A^* (f - A\varphi^{(b)}), \tag{1}$$

where f are measured data, $\varphi^{(b)}$ is some *first guess*, A is the operator mapping the system state into the measurements. The updated state $\varphi^{(a)}$ incorporates the knowledge which is gained from both the measurements and the first guess. The parameter $\alpha > 0$ reflects knowledge about the trust in the measurements and the first guess. The structure of this equation is very close to for example the regularized Newton scheme for inverse shape reconstruction, which searches the unknown shape φ by solving

$$\varphi_{k+1} - \varphi_k = (\alpha I + A'^* A')^{-1} A'^* (f - A\varphi_k), \quad k = 0, 1, 2, 3, ..., \tag{2}$$

where now A maps the shape into some scattered field measurements and A' denotes the derivative of the mapping A.

In the last part of the presentation we describe the general framework in which DA takes place in large operational centers like Deutscher Wetterdienst in contrast to a research environment at universities or companies. We picture development strategies, networking in Europe and beyond and the different research and development layers which need to be included into the process of numerical weather prediction.

References

[1] G. Evensen, Data Assimilation, The Ensemble Kalman Filter Springer Verlag 2009.
[2] B. Marx, Dynamic Magnetic Tomography, Dissertation, Göttingen 2010.
[3] B. Marx und R. Potthast, *On the Instability of Cycled Data Assimilation Methods*, (In Preparation).
[4] E. Kalnay, *Atmospheric Data Assimilation and Predictability*, Cambridge University Press 2004.
[5] W. Lahoz, B. Khattatov, R. Menard, Data Assimilation: Making Sense of Observations, Springer Verlag 2010.
[6] R. Potthast, *Point Source and Multipoles in Inverse Scattering Theory*, Chapman & Hall 2001.
[7] R. Potthast, *Convergence Criteria for Local Ensemble Filters*, (In Preparation).

An Iterative Approach to Probe Methods

Roland W.E. Potthast

Probe methods reconstruct some unknown shape from remote measurements by reconstructing some indicator function which has a special behaviour which characterizes the unknown shape. Such *direct* methods have been extremely popular over past years, compare [1]-[17]. For many methods the reconstruction of the indicator function needs some approximation domain which includes the unknown shape.

Here, we discuss three strategies to choose and update the approximation domain, i.e. the needle approach, domain sampling and as novel idea the LASSO scheme. It defines an iterative update which stopping rule to identify the unkonwn shape, for more details we refer to [10]. We discuss the algorithmical realization and the convergence analysis of the scheme. Numerical examples to prove its feasibility will be provided. The contraction of a curve in 2d which reconstructs four separate objects is shown in Figure 1.

References

[1] F. Cakoni and D. Colton (2006), Qualitative methods in inverse scattering theory. Springer Verlag.
[2] D. Colton, D. and A. Kirsch (1996), "A simple method for solving inverse scattering problems in the resonance region", Inverse Problems, vol. 12, no. 4, pp. 383-393.
[3] D. Colton and R. Kress (1998), Inverse acoustic and electromagnetic scattering theory, 2nd ed., ser. Applied Mathematical Sciences. Berlin: Springer-Verlag, vol. 93.
[4] M. Ikehata (1998), "Reconstruction of the shape of the inclusion by boundary measurements," Comm. PDE, vol. 23, pp. 1459-1474.

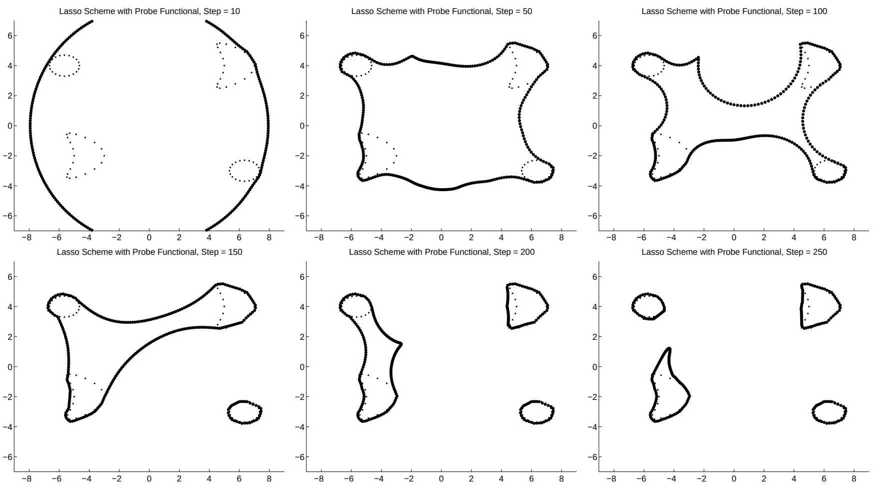

Figure 1. We show reconstruction steps 10, 50, 100, 150, 200, 250 when reconstructing an unknown object which has four separate components.

[5] A. Kirsch (1996), An introduction to the mathematical theory of inverse problems, ser. Applied Mathematical Sciences. New York: Springer-Verlag, vol. 120.

[6] A. Kirsch (1998), "Characterization of the shape of a scattering obstacle using the spectral data of the far field operator", Inverse Problems, vol. 14, no. 6, pp. 1489-1512.

[7] A. Kirsch and N. Grinberg (2008), The Factorization Method for Inverse Problems. Oxford Lecture Series in Mathematics & Its Applications.

[8] S. Kusiak, R. Potthast, and J. Sylvester (2003), "A range test for determining scatterers with unknown physical properties", Inverse Problems, vol. 19, no. 3, pp. 533-547.

[9] D. R. Luke and R. Potthast (2003), "The no response test - a sampling method for inverse scattering problems", SIAM Journal on Applied Mathematics, vol. 63, no. 4, pp. 1292-1312.

[10] R. Potthast (2010), An iterative framework for probe methods. Submitted for Publication.

[11] R. Potthast (2006), "A survey on sampling and probe methods for inverse problems", Inverse Problems, vol. 22, no. 2, pp. R1-R47.

[12] R. Potthast (2001), Point sources and multipoles in inverse scattering theory, ser. Chapman & Hall/CRC Research Notes in Mathematics. Chapman & Hall/CRC, Boca Raton, FL, vol. 427.

[13] R. Potthast (2000), "Stability estimates and reconstructions in inverse acoustic scattering using singular sources", J. Comput. Appl. Math., vol. 114, no. 2, pp. 247-274.

[14] R. Potthast and J. Schulz (2007), "A multiwave range test for obstacle reconstructions with unknown physical properties," Journal of Computational and Applied Mathematics, vol. 205, pp. 53-71.

[15] R. Potthast (1996), "A fast new method to solve inverse scattering problems", Inverse Problems, vol. 12, no. 5, pp. 731-742.

[16] R. Potthast (1998), "A point source method for inverse acoustic and electromagnetic obstacle scattering problems", IMA J. Appl. Math., vol. 61, no. 2, pp. 119-140.

[17] R. Potthast (2004), "A set-handling approach for the no-response test and related methods", Mathematics and Computers in Simulation, vol. 66, pp. 281-295.

Topological derivatives for inverse scattering problems

María-Luisa Rapún
(joint work with A. Carpio)

Numerical methods based on topological derivatives are powerful tools for inverse scattering problems associated with shape reconstruction and non–destructive testing. Recent work on topological derivatives focuses on problems where the nature of the scatterers is known [1, 5, 6]. We address here the full problem, developing strategies to reconstruct objects buried in a medium and their physical properties [3, 7]. The medium and the objects are illuminated by an incident radiation (electromagnetic, thermal, acoustic). The total field, composed of incident, scattered and transmitted waves, solves a transmission problem in the whole space. The inverse problem consists in reconstructing the objects and their material parameters from measurements of the total field at different locations.

For numerical purposes, inverse scattering problems are often reformulated as constrained optimization problems. One seeks domains and parameters minimizing the difference between the data measured at the detector locations and the total field associated to a given set of scatterers. Our strategy consists in generating a sequence of approximations for the domains and their parameters along which the cost functional decreases. Guesses of the objects are updated by adding regions in which the topological derivative of the cost functional is negative. This procedure provides good initial guesses of the scatterers without any a priori information about their shape or location. Each correction of the domains is followed by corrections of their parameters. Analytic expressions for such corrections are found computing the variations of the cost functional along particular directions. Formulae for the required topological derivatives and the parameter corrections were obtained in [3].

Reasonable reconstructions of the objects and their parameters are obtained in a few steps. Even if the predicted values of the parameters may deviate a bit from the exact ones due to noisy data, rough approximations are often useful to differentiate between different materials (in geophysics) or tissues (in biomedicine). Our techniques may be useful in digital image elasto–tomography for tumor detection [7, 8], for instance: healthy tissue, benign tumors and malignant tumors are known to have different stiffness constants.

We also explore the performance of the iterative method for the reconstruction of multiple sound–soft obstacles. In this case the reconstruction can be achieved (at least theoretically) by just a single incident wave [2]. Our numerical results show that accurate reconstructions of the number of obstacles and of their shapes can be obtained with one or a few incident waves.

Finally, we propose a new approach that combines the use of topological derivatives and Laplace transforms for shape reconstruction problems by thermal measurements in a time–dependent setting [4]. Numerical experiments show that thermal measurements allow for reasonable reconstructions of objects when they are placed near the surface and measurements are made on that surface during a well chosen time interval. A small number of sampling points or incident fields allow for good reconstructions if we measure the temperature many times: we obtain precise information on both the illuminated and shadow parts of the objects while considering the scattering of time–harmonic fields produce poorer results, specially in the shadow parts.

References

[1] M. Bonnet and A. Constantinescu, *Inverse problems in elasticity* Inverse problems **21** (2005), R1–R50.

[2] A. Carpio, B.T. Johansson, and M.-L. Rapún, *Determining planar multiple sound–soft obstacles from scattered acoustic fields* J. Math. Imaging Vis. **36** (2010), 185–199

[3] A. Carpio and M.-L. Rapún, *Solving inverse inhomogeneous problems by topological derivative methods* Inverse Problems **24** (2008), 045014

[4] A. Carpio and M.-L. Rapún, *Domain reconstruction using photothermal techniques* J. Comput. Phys. **227** (2008), 8083–8106

[5] G.R. Feijoo, *A new method in inverse scattering based on the topological derivative* Inverse Problems **20** (2004), 1819–1840

[6] B.B. Guzina and M. Bonnet, *Small-inclusion asymptotic of misfit functionals for inverse problems in acoustics* Inverse Problems **22** (2006), 1761–1785

[7] B.B. Guzina and I. Chikichev, *From imaging to material identification: A generalized concept of topological sensitivity* J. Mech. Phys. Solids **55** (2007), 245–279

[8] H.T. Liu, L.Z. Sun, G. Wang, and M.W. Vannier, *Analytic modeling of breast elastography* Med. Phys. **30** (2003), 2340–2349

K-REGINN: An inexact Newton regularization of Kaczmarz type

Andreas Rieder

(joint work with Antonio Leitão)

We like to solve the nonlinear ill-posed problem

$$F(x) = y^\delta \tag{1}$$

where $F\colon \mathsf{D}(F) \subset X \to Y$ operates between the real Hilbert spaces X and Y. Here, $\mathsf{D}(F)$ denotes the domain of definition of F. We further assume that problem (1) splits into $p \in \mathbb{N}$ 'smaller' subproblems, that is, Y factorizes into Hilbert spaces $Y_0, \ldots, Y_{p-1}$: $Y = Y_0 \times Y_1 \times \cdots \times Y_{p-1}$. Accordingly, $F = (F_0, F_1, \ldots, F_{p-1})^t$, $F_i\colon \mathsf{D}(F) \subset X \to Y_i$, and $y^\delta = (y_0^{\delta_0}, y_2^{\delta_1}, \ldots, y_{p-1}^{\delta_{p-1}})^t$.

Thus, (1) can be written as: find $x \in \mathsf{D}(F)$ such that

$$F_i(x) = y_i^{\delta_i}, \quad i = 0, \ldots, p-1. \tag{2}$$

The right hand sides $y_i^{\delta_i}$ are noisy versions of the exact but unknown data $y_i = F_i(x^+)$ satisfying

$$\|y_i - y_i^{\delta_i}\|_{Y_i} \le \delta_i.$$

The nonnegative *noise levels* δ_i are assumed to be known. Algorithm REGINN [3] for solving (1) is a Newton-type algorithm which updates the actual iterate x_n by adding a correction step s_n^{N} obtained from solving a linearization of (2):

$$x_{n+1} = x_n + s_n^{\mathrm{N}}, \quad n \in \mathbb{N}_0, \tag{3}$$

with an initial guess x_0. For obvious reasons we like to have s_n^{N} as close as possible to the exact Newton step

$$s_n^{\mathrm{e}} = x^+ - x_n.$$

Assuming F to be continuously Fréchet differentiable with derivative $F_i' \colon \mathsf{D}(F) \to \mathcal{L}(X, Y_i)$ the exact Newton step satisfies the linear equation

$$F_i'(x_n)s_n^{\mathrm{e}} = y_i - F_i(x_n) - E_i(x^+, x_n) =: b_{i,n}, \quad i = 0, \dots, p-1,$$

where

$$E_i(v, w) := F_i(v) - F_i(w) - F_i'(w)(v - w)$$

is the linearization error. In the sequel we will use the notation

$$A_{i,n} = F_i'(x_n).$$

Unfortunately, the above right hand sides $b_{i,n}$ are not available, however, we know perturbed versions

$$b_{i,n}^{\varepsilon} := y_i^{\delta_i} - F_i(x_n) \quad \text{with } \|b_{i,n} - b_{i,n}^{\varepsilon}\|_{Y_i} \le \delta_i + \|E_i(x^+, x_n)\|_{Y_i}.$$

Therefore, we determine the correction step s_n^{N} as a stable approximate solution of

$$A_{[n],n}s = b_{[n],n}^{\varepsilon} \tag{4}$$

where $[n] := n \mod p$ denotes the remainder of integer division. Stable approximate solutions of (4) are obtained by applying an iterative regularization scheme, called *inner iteration*, which can be written in the form

$$s_{[n],n,m} = s_{[n],n,m-1} + A_{[n],n}^* z_{[n],n,m-1}, \quad m = 1, 2 \dots, \quad s_{[n],n,0} = 0,$$

where $z_{i,n,m} \in Y_i$ determines the specific method. For instance, with $r_{i,n,m} = b_{i,n}^{\varepsilon} - A_{i,n}s_{i,n,m}$ being the residual we have that

- Landweber: $z_{i,n,m} = \omega r_{i,n,m}$, $\omega \in]0, \|A_{i,n}\|^{-2}[$,
- steepest decent: $z_{i,n,m} = \lambda_m r_{i,n,m}$, $\lambda_m = \dfrac{\|A_{i,n}^* r_{i,n,m}\|_X^2}{\|A_{i,n}A_{i,n}^* r_{i,n,m}\|_Y^2}$,
- implicit iteration: $z_{i,n,m} = (\alpha_m I + A_{i,n}A_{i,n}^*)^{-1} r_{i,n,m}$, $\alpha_m \in [\alpha_{\min}, \alpha_{\max}]$, $0 < \alpha_{\min} \le \alpha_{\max}$, and
- conjugate gradients: $z_{i,n,m} = w_{m+1}(A_{i,n}A_{i,n}^*, g)g$ for a polynomial $w_{m+1}(\cdot, g)$ of degree $m+1$.

Next we explain how to select the Newton step s_n^{N} from the regularizing sequence $\{s_{[n],n,m}\}_m$. Choose $R > 1$ and set

$$s_n^{\mathrm{N}} := \begin{cases} s_{[n],n,m_n} : \|b_{[n],n}^{\varepsilon}\|_{Y_{[n]}} > R\delta_{[n]}, \\ s_{[n],n,0} : \quad \text{otherwise}, \end{cases}$$

where

$$m_n = \min\left\{m \in \mathbb{N} : \|A_{[n],n}s_{[n],n,m} - b_{[n],n}^{\varepsilon}\|_{Y_{[n]}} < \mu_n \|b_{[n],n}^{\varepsilon}\|_{Y_{[n]}}\right\}$$

for a picked tolerance $\mu_n \in]0, 1]$.

Finally, we stop the Newton iteration (3) as soon as it is constant over a full cycle, i.e., the iterate $x_{N(\delta)}$ is accepted as approximation to x^+ if

$$x_{N(\delta)} = x_{N(\delta)+1} = \cdots = x_{N(\delta)+p}.$$

Written differently we have

$$N(\delta) = \min\big\{n \in \mathbb{N} \,:\, x_n = x_{n+1} = \cdots = x_{n+p}\big\}.$$

Hence, the final iterate satisfies the discrepancy principal for all subproblems:

$$\big\|y_i^{\delta_i} - F_i(x_{N(\delta)})\big\|_{Y_i} \le R\delta_i, \quad i = 0, \ldots, p-1. \tag{5}$$

We call the resulting procedure `K-REGINN` (Kaczmarz-type REGINN), see, e.g., [1, 2] for other Kaczmarz-type iterations.

For our convergence analysis we assume the tangential cone condition: there is a positive $L < 1$ such that, for all $v, w \in B_r(x^+) \subset \mathsf{D}(F)$ and $i = 0, \ldots, p-1$,,

$$\|E_i(v,w)\|_Y \le L\|F_i'(w)(v-w)\|_Y.$$

Theorem: *Let $F\colon \mathsf{D}(F) \subset X \to Y$ be completely continuous. Assume one of the four inner iterations from above is used in* `K-REGINN`. *Further, let R be sufficiently large, L sufficiently small and choose the tolerances $\{\mu_n\}$ within a certain closed interval in $]0,1[$.*

If $x_0 \in B_r(x^+)$ then there exists an $N(\delta)$ such that all iterates $\{x_1, \ldots, x_{N(\delta)}\}$ of `K-REGINN` *are well defined and stay in $B_r(x^+)$. We even have a strictly monotone error and residual reduction: if $x_n \neq x_{n+1}$ then*

$$\|x^+ - x_{n+1}\|_X < \|x^+ - x_n\|_X \tag{6}$$

and there is a $\Lambda < 1$ independent of n such that

$$\big\|y_{[n]}^{\delta_{[n]}} - F_{[n]}(x_{n+1})\big\|_{Y_{[n]}} < \Lambda\big\|y_{[n]}^{\delta_{[n]}} - F_{[n]}(x_n)\big\|_{Y_{[n]}}.$$

Moreover, only the final iterate satisfies the discrepancy principle (5).

Corollary: *Let the assumptions of above theorem hold true. Moreover, given a sequence $\{\delta^j\}_{j\in\mathbb{N}} \subset \mathbb{R}_+^p$ with $\lim_{j\to\infty} \delta^j = 0$, let $\{x_{N(\delta^j)}\}_{j\in\mathbb{N}}$ be the corresponding elements generated by* `K-REGINN`.

Then, any subsequence of $\{x_{N(\delta^j)}\}_{j\in\mathbb{N}}$ contains a subsequence which converges weakly to a solution of the system $F_i(x) = y_i$, $i = 0, \ldots, p-1$. Moreover, if x^+ is the only solution in $B_r(x^+)$ then the whole sequence $\{x_{N(\delta^j)}\}_{j\in\mathbb{N}}$ converges weakly to x^+.

In the remainder we discuss shortly our approach to prove strong convergence. Subsequently, we need to differ clearly between the noisy ($\delta > 0$) and the noiseless ($\delta = 0$) situations: Iterates with a superscript δ refer to the noisy setting ($y^\delta \neq y$), those without superscript refer to exact data y. To prove $\lim_{j\to\infty} \|x^+ - x_{N(\delta^j)}^{\delta^j}\|_X = 0$ if x^+ is the unique solution in $B_r(x^+)$ we try to follow an established modus operandi, see, e.g., [1, 2]:

(1) Show convergence for unperturbed data: $\lim_{n\to\infty} x_n = x^+$.
(2) Show stability: $\lim_{\delta\to 0} x_n^\delta = x_n$.

(3) Employ triangle inequality: for $m \leq N(\delta)$, by (6) we have that

$$\|x^+ - x^\delta_{N(\delta)}\|_X \leq \|x^+ - x^\delta_m\|_X \leq \|x^+ - x_m\|_X + \|x_m - x^\delta_m\|_X.$$

At the moment we investigate convergence for unperturbed data utilizing square summability of the nonlinear residuals, that is,

$$\sum_{i=0}^{\infty} \|y_{[i]} - F_{[i]}(x_i)\|^2_{Y_{[i]}} \lesssim \|x^+ - x_0\|^2_X.$$

References

[1] J. Baumeister, B. Kaltenbacher, and A. Leitão, *On Levenberg-Marquardt-Kaczmarz iterative methods for solving systems of nonlinear ill-posed equations*, Inverse Probl. Imaging **4** (2010), pp. 335–350.

[2] R. Kowar and O. Scherzer, *Convergence analysis of a Landweber-Kaczmarz method for solving nonlinear ill-posed problems*, Ill-Posed and Inverse Problems (V.G. Romanov et al. eds.) (2002), VSP Zeist, pp. 69–90.

[3] A. Lechleiter and A. Rieder, *Towards a general convergence theory for inexact Newton regularizations*, Numer. Mathematik **114** (2010), pp. 521–548.

Reporter: Corinna Burkard

Participants

Dr. Corinna Burkard
Institut Elie Cartan
-Mathematiques-
Universite Henri Poincare, Nancy I
Boite Postale 239
F-54506 Vandoeuvre les Nancy Cedex

Prof. Dr. Marc Dambrine
Lab. de Mathematiques Appliquees
Universite de Pau et des Pays de l'Adour
BP 1155
F-64013 Pau Cedex

Prof. Dr. Eric G. Darrigrand
U. F. R. Mathematiques
I. R. M. A. R.
Universite de Rennes I
Campus de Beaulieu
F-35042 Rennes Cedex

Dr. Thomas Fidler
Fakultät für Mathematik
Universität Wien
Nordbergstr. 15
A-1090 Wien

Prof. Dr. Helmut Harbrecht
Institut für Angewandte Analysis
und Numerische Simulation
Universität Stuttgart
Pfaffenwaldring 57
70569 Stuttgart

PD Dr. Frank Hettlich
Fakultät für Mathematik
Karlsruher Institut für Technologie(KIT)
76128 Karlsruhe

Prof. Dr. Barbara Kaltenbacher
Institut für Mathematik
Karl-Franzens-Universität Graz
Heinrichstr. 36
A-8010 Graz

Prof. Dr. Andreas Kirsch
Fakultät für Mathematik
Karlsruher Institut für Technologie(KIT)
76128 Karlsruhe

Dr. Frederique Le Louer
Institut für Numerische
und Angewandte Mathematik
Universität Göttingen
Lotzestr. 16-18
37083 Göttingen

Dr. Armin Lechleiter
Ecole Polytechnique/INRIA Saclay
CMAP UMR 7640 CNRS
F-91128 Palaiseau Cedex

Prof. Dr. Gen Nakamura
Department of Mathematics
Hokkaido University
Kita-ku
Sapporo 060-0810
JAPAN

Prof. Dr. Roland Potthast
Department of Mathematics
University of Reading
Whiteknights
P.O.Box 220
GB-Berkshire RG6 6AX

Dr. Maria-Luisa Rapun
Dpto. Fundamentos Matematicos
E.T.S.I. Aeronauticos
Universidad Politecnica de Madrid
Plaza Cardenal Cisneros 3
E-28040 Madrid

Prof. Dr. Andreas Rieder
Karlsruher Institut f. Technologie (KIT)
Inst. f. Angew. & Numerische Mathematik
76128 Karlsruhe